ABSTRACT

Title of thesis: JOINT ENERGY BEAMFORMING AND TIME ASSIGNMENT FOR COOPERATIVE WIRELESS POWERED NETWORKS

Chen Chen, Master of Science, 2016

Thesis directed by: Professor Gang Qu
Department of Electrical and Computer Engineering

Wireless power transfer (WPT) and radio frequency (RF)-based energy harvesting arouses a new wireless network paradigm termed as wireless powered communication network (WPCN), where some energy-constrained nodes are enabled to harvest energy from the RF signals transferred by other energy-sufficient nodes to support the communication operations in the network, which brings a promising approach for future energy-constrained wireless network design.

In this paper, we focus on the optimal WPCN design. We consider a network composed of two communication groups, where the first group has sufficient power supply but no available bandwidth, and the second group has licensed bandwidth but very limited power to perform required information transmission. For such a system, we introduce the power and bandwidth cooperation between the two groups so that both group can accomplish their expected information delivering tasks. Multiple antennas are employed at the hybrid access point (H-AP) to enhance both energy and information transfer efficiency and the cooperative relaying

is employed to help the power-limited group to enhance its information transmission throughput. Compared with existing works, cooperative relaying, time assignment, power allocation, and energy beamforming are jointly designed in a single system. Firstly, we propose a cooperative transmission protocol for the considered system, where group 1 transmits some power to group 2 to help group 2 with information transmission and then group 2 gives some bandwidth to group 1 in return. Secondly, to explore the information transmission performance limit of the system, we formulate two optimization problems to maximize the system weighted sum rate by jointly optimizing the time assignment, power allocation, and energy beamforming under two different power constraints, i.e., the fixed power constraint and the average power constraint, respectively. In order to make the cooperation between the two groups meaningful and guarantee the quality of service (QoS) requirements of both groups, the minimal required data rates of the two groups are considered as constraints for the optimal system design. As both problems are non-convex and have no known solutions, we solve it by using proper variable substitutions and the semi-definite relaxation (SDR). We theoretically prove that our proposed solution method can guarantee to find the global optimal solution. Thirdly, consider that the WPCN has promising application potentials in future energy-constrained networks, e.g., wireless sensor network (WSN), wireless body area network (WBAN) and Internet of Things (IoT), where the power consumption is very critical. We investigate the minimal power consumption optimal design for the considered cooperation WPCN. For this, we formulate an optimization problem to minimize the total consumed power by jointly optimizing the time assignment, power allocation,

and energy beamforming under required data rate constraints. As the problem is also non-convex and has no known solutions, we solve it by using some variable substitutions and the SDR method. We also theoretically prove that our proposed solution method for the minimal power consumption design guarantees the global optimal solution. Extensive experimental results are provided to discuss the system performance behaviors, which provide some useful insights for future WPCN design. It shows that the average power constrained system achieves higher weighted sum rate than the fixed power constrained system. Besides, it also shows that in such a WPCN, relay should be placed closer to the multi-antenna H-AP to achieve higher weighted sum rate and consume lower total power.

JOINT ENERGY BEAMFORMING AND TIME ASSIGNMENT FOR COOPERATIVE WIRELESS POWERED NETWORKS

by

Chen Chen

Thesis submitted to the Faculty of the Graduate School of the
University of Maryland, College Park in partial fulfillment
of the requirements for the degree of
Master of Science
2016

Advisory Committee:
Professor Gang Qu, Chair/Advisor
Professor Manoj Franklin
Professor Sennur Ulukus

Acknowledgments

First and foremost I owe my gratitude to my advisor, Professor Gang Qu for his guidance and perspective on my thesis. Those viewpoints turn out to be inspirational and insightful along the process. His extreme patience also makes me feel motivated during the process.

Next, I am also grateful for Dr. Ke Xiong, who is knowledgeable and willing to discuss. The thesis would be impossible without his endeavor. It is a pleasure to learn from a patient and encouraging person like him.

Many thanks to Professor Manoj Franklin and Professor Sennur Ulukus for their valuable time on serving as my thesis committee and reviewing the manuscript.

Finally, I owe my thanks to my family. They are always supportive along the way no matter what. Thank you all!

Table of Contents

List of Figures

List of Abbreviations

RF	Radio Frequency
WPT	Wireless Power Transfer
SWIPT	Simultaneous Wireless Information and Power Transfer
DF	Decode-and-forward
AF	Amplify-and-forward
EB	Energy Beamforming
WSR	Weighted sum rate
EH	Energy Harvesting
QoS	Quality-of-service
H-AP	Hybrid Access Point
FD	Full Duplex
RFID	Radio Frequency Identification
WPC	Wireless Power Communication
WPCN	Wireless Power Communication Network
DL	Downlink
UL	Uplink
FSK	Frequency-shift Keying
EM	Electromagnetic
MIMO	Multiple-Input Multiple-Output
LPF	Low-pass Filter
AWGN	Additive White Gaussian Noise
MISO	Multiple-Input Single-Output

Chapter 1: Introduction

1.1 Background

In the last decade, the popularization of wireless applications has been increasing greatly due to the fast development of various wireless technologies. Nevertheless, energy supply to wireless devices still continues as an important constraint in wireless networks, especially for energy-constrained networks, such as wireless sensor networks (WSNs), wireless personal area networks (WPANs), wireless body networks (WBANs) and Internet of Things (IoT), which have a limited lifetime, largely confining the network performance [1–6].

To relieve this problem, there are two effective ways. One is the energy-efficient communication system design [7–9], in which the efficiency of the per-unit energy consumption (e.g., the amount of information can be transferred per Joule) is maximized or the power consumption is minimized while guaranteeing the required minimal information rate of the users. Another is to employ energy harvesting (EH) technologies [10–16], by which electricity energy can be harvested and converted from various ambient energy sources such as solar, wind, vibration, and temperature. As a promising idea, EH instruments can be applied to supply power for wireless devices, acting as green energy sources. As a matter of fact, it is possible to

use one or more of these sources to provide a stable energy supply according to practical application conditions. However, the usage of these energy sources has some challenges and limitations due to their availability in natural environment. Moreover, as nature sources are uncontrollable, nature energy source based EH techniques sometimes are not capable of providing stable and continuous power supply.

As an alternative, it is also possible to harvest energy from radio frequency (RF) signals, as RF signals also carry energy [4]. RF-based EH allows wireless devices to harvest energy from RF signals for their information processing and transmission, where RF signal is captured at the receiver and then converted into direct current signal by energy conditioning circuit. These current signals are later used to power the target device, e.g., stored into a battery or a super-capacitor. Compared with traditional nature source based EH techniques, there are some merits of the RF-based EH techniques. Firstly, RF signals can be manually designed and controlled, which has much less dependency on environment, so it is able to provide stable and adjustable energy supply. Secondly, ambient RF signals can be gathered from all wireless communication nodes including cellular base stations, access points, television towers, radio broadcast stations, and mobile user devices, which provide abundant energy sources. Since the power density at the receiver depends on the transmit power at the sources and the wireless signal propagation distance, RF energy is predictable if an intended EH receiver is static. It was reported that a power station transmitting tens of watts is capable of powering sensors, smartphones, laptops at a distance less than 15 m [1]. Moreover, although ambient RF signals are free and sufficient in urban areas, it is scarce in suburb areas. There-

fore, as a strong supplement, the dedicated RF energy sources like cellular power towers are able to provide on-demand energy supply with Quality-of-service (QoS) constraints. Owing to its potential applications in various energy-constrained networks, the Wireless Power Consortium has began to make efforts on establishing an international standard for the RF-based EH technique.

A significant application of RF-based EH is wireless powered communication (WPC) [2,3], in which energy is transferred via RF signals between power-sufficient nodes and power-constrained nodes. The power-constrained devices are able to use the harvested RF energy to transmit/decode information to/from others. As energy can be harvested from the continuously transmitted signals, the communication is not interrupted by energy depletion. So, WPC is capable of improving user experience and convenience with higher and more sustainable information transmission performance than traditional battery-powered communication. On account of the high attenuation of signal (or microwave) energy over distance, RF-based EH is more suitable to be used for supporting low-power devices including low-power sensors and RFID tags. Thanks to recent development in antenna technology and RF-based EH circuit, wireless devices are enabled to transfer and harvest much higher microwave power [6]. Therefore, it is expected that WPC will be an important building block in many popular commercial and industrial networks in the future, such as large-scale WSNs and the upcoming IoT consisting of billions of sensing/RFID nodes.

As is known, information is also transmitted by wireless signals, so it can be jointly transmitted with energy via the same signal, which is referred to as the simultaneous wireless information and power transfer (SWIPT) [17–19] and it was

proved to be more efficient in spectrum usage than transmitting information and energy over orthogonal frequency or time channels. It has become an important way to transfer energy and power the devices in WPC systems.

1.2 Related work

So far, WPC network (WPCN) has attracted increasing interest. In [20], a single-antenna hybrid access point (H-AP)-assisted WPCN was investigated, where the H-AP is with steady energy supply and it first transfers energy to a group of users and then the users transmit information to the H-AP by using the harvested energy. The total throughput of all users were maximized by optimally assigning the time slots. In [21], a two-user single-antenna H-AP-assisted WPCN was considered. Different from [20], in [21], the user cooperation between the two users was considered and the weighted sum-rate (WSR) was maximized by jointly optimizing the time assignment and power allocation.

Since beamforming technology is able to focus the transmitted energy on a specific receiver, in order to improve the energy transmission efficiency, some works began to consider energy beamforming in WPCNs. In [22], energy beamforming was optimally designed for a point-to-point multi-antenna WPCN, in which a multi-antenna transmitter emitted energy to a receiver to drive the information transmission of the receiver. In [23], joint energy beamforming design and time allocation was investigated to maximize the sum rate of multiple users in a WPCN, where the users harvest energy from a power station and then use the harvested energy to

transmit information to their destinations, respectively.

Besides, in [25], a large-scale WPCN was studied, where the stochastic geometry was used to analyze the wireless nodes performance tradeoff between energy harvesting and information transmission. In [24], the optimal resource allocation was designed for the WPCN, where one H-AP operating in full duplex (FD) broadcasts wireless energy to a set of distributed users in the downlink (DL) and, at the same time, receives independent information from the users via time-division multiple access (TDMA) in the uplink (UL). In [26], a backscatter radio based WPCN was studied, where users harvest energy from both the signal broadcasted by the H-AP and the carrier signal transmitted by the carrier emitter in the downlink and transmit their own information in a passive way via the reflection of the carrier signal using frequency shift keying (FSK) modulation in the uplink. In [27], the authors studied a multi-antenna WPCN with cochannel energy and information transfer, where a wireless device, powered up by wireless energy transfer (WET) from an energy transmitter, communicates to an information receiver over the same frequency band, where the achievable data rate from the wireless device to the information receiver was maximized by jointly optimizing the energy beamforming at the energy transfer and the information beamforming at the wireless device, subject to their individual transmit power constraints. In [28], the maximum network energy efficiency was explored by joint time allocation and power control while taking account the initial battery energy level of each user. In [29], the authors investigated the optimal resource allocation in a power beacon-assisted WPCN to maximize the system weighted sum rate. In [30], the delay-aware WPCN was investigated, where the

delay-aware energy balancing was presented by minimizing the average transmission delay while taking into account theissue of unbalanced harvested energy distribution. In [31], the placement optimization of energy and information access points in WPCNs was investigated, where the wireless devices harvest the radio frequency energy transferred by dedicated energy nodes in the downlink, and use the harvested energy to transmit data to information access points (APs) in the uplink, where the number of energy nodes and APs was minimized by optimizing their locations, while satisfying the energy harvesting and communication performance requirements of the wireless devices. In [32], a three-node WPCN was studied, where a power receiver harvests energy from a wireless power transmitter via wireless power transfer in the downlink and then executes information transfer in the uplink. The system throughput was maximized by balancing the time duration between the wireless power transfer phase and the information transfer phase while satisfying the energy causality constraint. In [33], a multiuser WPCN was considered, where energy constrained users charge their energy storages by scavenging energy of the radio frequency signals radiated from an H-AP. The uplink sum rate was maximized by jointly optimizing energy and time resource allocation for multiple users in both infinite capacity and finite capacity energy storage cases. In [34], the authors investigated work for WPCN OFDM systems, where an H-AP broadcasts energy signals to users in the downlink, and the users transmit information signals to the H-AP in the uplink based on orthogonal frequency division multiple access. A joint subcarrier scheduling and power allocation was designed to maximize the system sum-rate. In [35], a harvest-use-store power splitting (PS) relaying strategy with distributed

beamforming was proposed for WPCN, where harvested energy was assumed to be prioritized to power information relaying while the remainder was accumulated and stored for future usage with the help of a battery in the proposed strategy, which may support an efficient utilization of harvested energy.

1.3 Motivation & Contribution

As described in Section 1.2, many works on WPCNs can be found in the literature. However, as a newly emerged wireless communication system, WPCN still has many fundamental issues to be studied. For example, some existing works considered the point-to-point communications in WPCNs, see e.g., [20,25,27,31], where however, no relaying was involved. Although some works designed the transmission strategy for relay-aided cooperative systems, see e.g., [21, 26, 35], all nodes were assumed to be equipped with single antenna, where no multi-antenna technology was considered. As time, bandwidth and power are limited resources for wireless systems, some existing works began to investigate the system performance limits in terms of sum-rate and weighted sum-rate for various WPCNs by introducing resource allocations. Nevertheless, some of them only discussed one or two kinds of resources, see e.g., [22–24, 28–30, 32–34]. Multiple resources were not jointly optimized in a single system for better system performance. More importantly, most of current works did not consider the cooperation between different communication pairs in the WPCNs.

In this paper, we also focus on the WPCN system. We consider a network

composed of two communication groups, where the first group has sufficient power supply but no available bandwidth, and the second group has licensed bandwidth but very limited power to perform required information transmission. As cooperation (including information cooperation and energy cooperation[1]) is available and sometimes very critical in wireless systems, we introduce the power and bandwidth cooperation between the two groups so that both group can accomplish their expected information delivering tasks. Compared with existing works, cooperative relaying, time assignment, power allocation, and energy beamforming are jointly designed in a single system.

The contributions of our work are summarized as follows.

Firstly, we propose a cooperative transmission protocol for the considered system, where group 1 transmits some power to group 2 to help group 2 with information transmission and then group 2 gives some bandwidth to group 1 in return.

Secondly, to explore the information transmission performance limit of the system, we formulate two optimization problems to maximize the system weighted sum rate (WSR) by jointly optimizing the time assignment, power allocation, and energy beamforming under different power constraints, i.e., the fixed power constraint and the average power constraint. In order to make the cooperation between the two groups meaningful and guarantee QoS requirements of both groups, the minimal required data rates of the two groups are also considered as constraints for the opti-

[1]The wireless power transfer makes the energy cooperation implementable in practical systems and the SWIPT technique makes joint information and energy cooperation practical for WPCNs

mal system design. As both problems are non-convex and have no known solutions, we solve it by using proper variable substitution and the semi-definite relaxation (SDR). We theoretically prove that our proposed solution method can guarantee to find the global optimal solution.

Thirdly, consider that the WPCN has promising application potentials in future energy-constrained networks, where the power consumption is very critical. We investigate the minimal power consumption optimal design for the considered cooperation WPCN. For this, we formulate an optimization problem to minimize the total consumed power by jointly optimizing the time assignment, power allocation, and energy beamforming under required data rate constraints. As the problem is also non-convex and has no known solutions, we solve it by using some variable substitutions and the SDR method. We also theoretically prove that our proposed solution method for the minimal power consumption design guarantees the global optimal solution.

Fourthly, extensive experimental results are provided to discuss the system performance behaviors, which provide some useful insights for future WPCN design. It shows that the average power constrained system achieves higher WSR than the fixed power constrained system. Besides, it also shows that in such a WPCN, relay should be placed closer to the multi-antenna H-AP to achieve higher weighted sum rate and consume lower total power.

1.4 Organization

The rest of the thesis is organized as follows. In Chapter 2, some related conceptions and technologies are introduced for better understanding of our work. In Chapter 3, the system model is described and the transmission protocol is presented. In Chapter 4, we consider the WSR design of our considered WPCN, where the fixed power scenario and the average power constrained scenario are studied. In Chapter 5, the minimal power optimization design of our system is investigated. Finally, Chapter 6 summarizes our work and also suggest some future work.

Chapter 2: Preliminary Conceptions

2.1 Wireless Power Transfer

By leveraging the far-field radiative properties of electromagnetic (EM) waves, wireless receivers could harvest energy remotely from RF signals radiated by an energy transmitter, which is also referred to as wireless power transfer (WPT) [36].

Although WET has attracted high popularity recently, its related research work can be traced back to more than a century ago. Three different kinds of existing WET technologies have been proposed, i.e., inductive coupling, magnetic resonant coupling, and EM radiation. Among them, the first two types utilize the non-radiative near-field EM properties provided by an antenna for short-range high-power transfer. Particularly, inductive coupling WET is currently well standardized, which is used to charge mobile phones and implanted medical devices. Due to the drastic drop in magnetic induction effect over distance, inductive coupling only operates within a range of only several centimeters. Compared with the inductive coupling, magnetic resonant coupling WET has much wider operating range, which reaches a few meters. However, in the magnetic resonant coupling WET systems, the receiver has to be positioned at a specific place, as it must be optimized for some fixed distance and circuit alignment settings in order to maintain resonant

coupling. Moreover, it is also difficult to use magnetic resonant coupling WET to power multiple devices as it requires careful tuning to avoid interference caused by the mutual coupling effect. Comparably, EM radiation is able to power wireless devices over moderate to long distances. RF-based EH or RF-based WET exploits the far-field radiative properties of EM radiation.

It was reported that a typical RFID tag with around 0.5 mW received RF power could be powered from 4m away, and some RF EH chips with around 0.05 mW received RF power can reach a maximum 12-14 m line-of-sight operating radius. With RF-based EH, RF energy receivers can be flexibly positioned and made very tiny to fit into commercial devices. Moreover, transferring energy to multiple devices becomes easily owing to the broadcasting property of wireless channels. The major limitation of RF-based WET is the high EM energy attenuation over distance. Nonetheless, with the multiple-input multiple-output (MIMO) transmission technology, wireless energy transfer efficiency can be greatly enhanced. Additionally, the device operating power (as low as a few microwatts for some RFID tags) is continuously being decreased. Therefore, RF-EH technology is expected to be applied to deployed in various wireless systems.

As illustrated in Figure 2.1, the RF-based EH receiver contains a rectifying circuit, consisting of a diode and a passive low-pass filter (LPF), which is able to convert received RF signals to DC signals to charge the built-in battery, which stores the energy. Following the law of energy conservation, the harvested energy P_h is

proportional to the received RF power P_r, which can be expressed by

$$P_h = \eta P_r = \eta \frac{P_t G}{d^\alpha}, \tag{2.1}$$

where $\eta \in (0, 1)$ denotes the overall energy conversion efficiency at the receiver. P_t is the transmit power and d is the distance between the energy transmitter and its receiver. α denotes the path loss factor and G represents the combined antenna gain of the transmit and receive antennas.

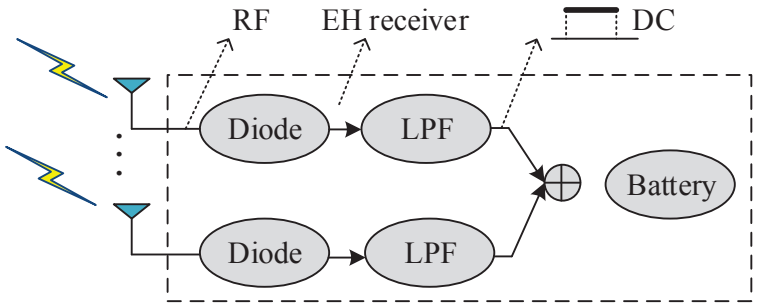

Figure 2.1: RF-based EH receiver architecture.

It was reported that, with two-antenna configuration at both the transmitter and the receiver, a beamforming gain to increase the harvested energy by about four times (6 dB) compared to the case with a singleantenna transmitter and receiver with the same transmission power. This could be more cost effective in practice than the alternative approach of improving the energy conversion efficiency (say, from 25 to 99 percent), at the receiver with more sophisticated designs of rectifying circuits.

2.2 Energy Beamforming

Eq. (2.1) shows that increasing G can raise the harvested energy P_h. So the one way is to explore new efficient antenna design technology to improve G. Besides, another effective way to improve G is employing multi-antenna technology. In fact, with multiple antennas, on one hand, the antenna power gain can be enhanced by exploiting diversity gains. On the other hand, energy beamforming techniques can be realized to focus the transmit power in a smaller region of space to bring significant improvement to energy transfer efficiency.

By properly design the waveform transmitted at each antenna, energy beamforming is capable of adjusting the radiated waveforms such that they could be combined at a specific receiver coherently. Generally, the larger number of antennas equipped at the energy transmitter, the sharper energy beam could be generated focusing on a spatial direction.

2.3 SWIPT

Since RF signals which carry energy at the same time can also be used as a carrier for information delivering, SWIPT has become an interesting research topic, which attracts increasing attention.

SWIPT is able to save spectrum via transmitting energy and information jointly with the same waveform or signals. However, SWIPT involves a rate-energy trade-off at both the transmitter and receiver to balance the information decod-

ing (ID) and EH performance. At the transmitter side, waveforms are generated to determine the performance of information and energy transfer. In a extreme case, the transmitter may ignore energy (or information) receivers and optimize the waveforms only to maximize information (or energy) transmission efficiency. Nevertheless, because of the fundamental difference in the optimal waveforms for energy and information transmissions, such an off-balance design possibly leads to a poor performance of either energy and information transmission. Therefore, the waveform are required to be designed following a rate-energy trade-off to achieve the best balance between the energy and information transfer [19]. On the other hand, the performance of SWIPT is also closely related to the receiver's structure and the corresponding signal processing schemes [19, 37]. Although related study on SWIPT is still in the infancy stage, some notable results were reported in the literature [17, 18]. For example, at first, an ideal SWIPT receiver was assumed to be able to decode information and harvest energy from the same signal with the same circuit [17]. Later, it was pointed out that [19] such an assumption cannot be realized in practical systems. Therefore, several practical receiver structures, e.g., time switching (TS), power splitting (PS), integrated ID/EH receiver (IntRx), and antenna switching (AS) were proposed in [19].

2.4 Cooperative Communication

In cooperative communications, a source transmits a message to a destination with the assistance of one or more relays. Conventionally, relaying was used to

extend the range of wireless communication systems. In recent years, many applications of relaying were proposed [38]. One of them is to use relay node to assist in the communication between the source and its destinations via some cooperation protocols, which is termed as cooperative relaying. So far, cooperative relaying has emerged as a promising approach to combat fading in wireless networks in order to achieve cooperative diversity gain, by which the system throughput and communication reliability can be enhanced. At the same time, the power consumption can also be greatly reduced.

In [38], two well-known cooperative relaying strategies, i.e., amplify-and-forward (AF) and decode-and-forward (DF) were proposed. In AF relaying strategy, the relay sends an amplified version of the received signal from the source to the destination. While in DF relaying strategy, the relay decodes the source message in one block and transmits the re-encoded message in the following block. Comparing with AF, DF relaying avoids forwarding the noise received over the source-relay link to the destination, so it has better system performance than AF relaying, especially when the source-relay link is with good channel condition. There have been a great deal of ongoing research on developing cooperative relaying protocols and resource management methods to exploit the potential benefits of cooperative relaying [38–40].

Notations: $\mathbb{C}^{M\times N}$, $\mathbb{H}^{M\times N}$, $\mathbb{R}^{M\times N}$ denote the set of complex, Hermitian and real matrices with size of M rows and N columns, respectively. $\|\cdot\|$ denotes the Frobenius norm. $\mathrm{Tr}(\mathbf{X})$ is the trace of matrx $\mathbf{X}$.

Chapter 3: System Model

3.1 Network Model

We consider a wireless system consisting of five nodes, i.e., two source nodes S_1 and S_2, two destination nodes D_1 and D_2 and one relay node R, as illustrated in Figure 3.1. S_1 desires to transmit information to D_1 while S_2 desires to transmit information to D_2. It is assumed that S_1 is with stable and sufficient power supply but no licensed bandwidth for information transmission to D_1. Meanwhile S_2 has licensed bandwidth but it is located relatively far away from D_2, so reliable high data rate transmission can not be achieved over the $S_2 \rightarrow D_2$ direct link. Thus the information transmission from S_2 to D_2 needs help from R. However, R could not participate in the information transmission due to some reasons. For example, R is an energy exhausted node and has no available power or it is a selfish node who is powered by battery and it is not willing to consume its own power to help other nodes. We refer (S_1, D_1) as the group 1 communication unit and (S_2, R, D_2) as the group 2 communication unit. That is, group 1 has sufficient power but no bandwidth while group 2 has sufficient bandwidth but limited power. So each of them cannot achieve desired information delivery purpose. In this case, the two groups may cooperate with each other in terms of power and bandwidth to achieve

a "win-win" outcome to fulfill their respective information transmission requirements. Specifically, S_1 may transmit some power to R to enable R participating the information transmission between S_2 and D_2. In return, S_2 may bestow a portion of its bandwidth to S_1. Via the cooperation, both groups may successfully delivery their information.

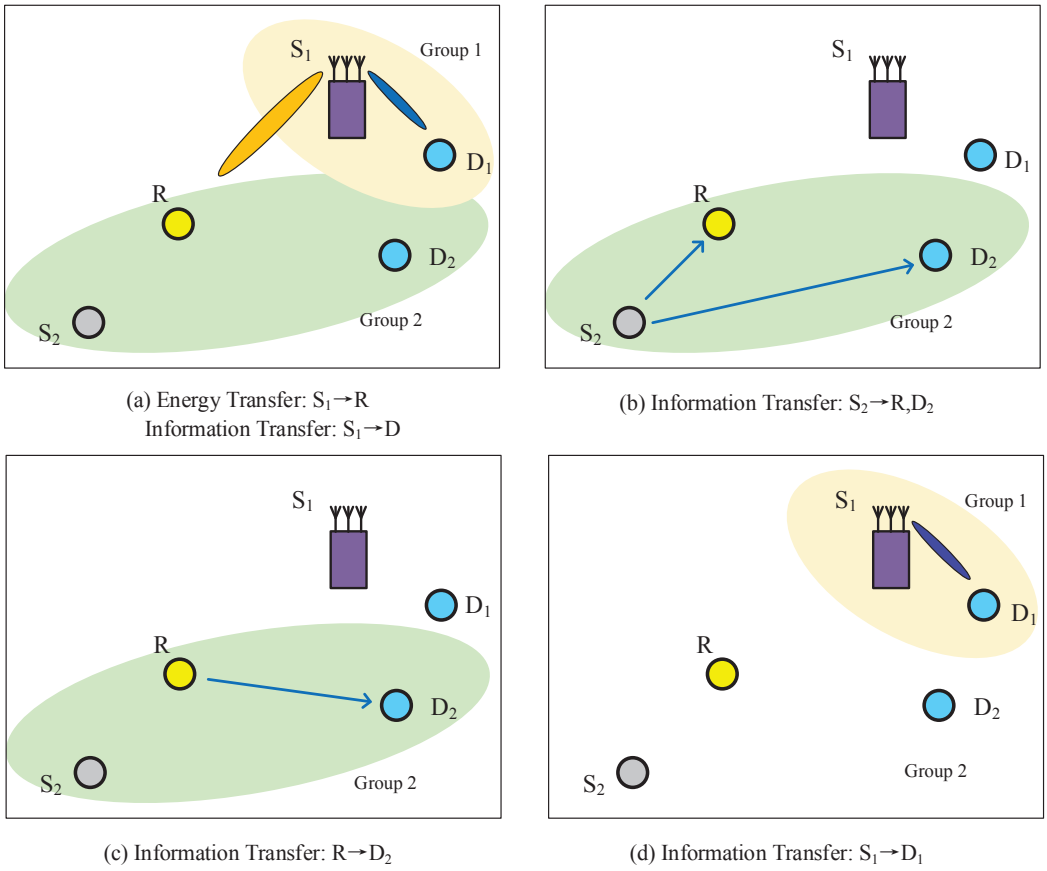

Figure 3.1: System model.

Such a communication scenario can be found in many different wireless systems. For example, in WSNs and cognitive networks. In order to enhance the energy transfer efficiency, S_1 is assumed to be equipped with N antennas while all other nodes only support single antenna due to their size limitations. Block fading channel

is considered, so that all channel coefficients can be regarded as constants during each fading block and vary from block to block independently, following Rayleigh distribution. $h_{ij}(k)$ is used to denote the channel coefficient of the k-th block between node i and node j. $n(k) \sim \mathcal{CN}(0, N_0)$ is the Additive White Gaussian Noise (AWGN) of the k-th block. So, $h_{ij}(k) \sim \mathcal{CN}(0, d_{ij}^{-\alpha})$, where d_{ij} is the distance between node i and node j, α is the path loss exponent factor. The time period of each fading block is denoted with T.

3.2 Transmission Protocol

To complete cooperation transmission, each time period T is divided into four phases, which are with time intervals of τ_1, τ_2, τ_3 and τ_4, respectively. Without loss of generality, T is normalized to 1 in the sequel, so that $\sum_{i=1}^{4} \tau_i = 1$ and $\tau_i \geq 0$. Defining $\boldsymbol{\tau} \triangleq [\tau_1 \ \tau_2 \ \tau_3 \ \tau_4]^T$, which can be regarded as the time assignment vector of the four transmission phases, we know that it satisfies

$$\mathbf{1}^T \boldsymbol{\tau} = 1, \ \boldsymbol{\tau} \succeq \mathbf{0}, \tag{3.1}$$

where $\mathbf{1}$ is a column vector with all elements being 1.

In the first phase, S_1 transfers energy to R and transmits information to D_1 simultaneously. Let $x_{S_1}(k)$ with $|x_{S_1}(k)|^2 = 1$ be the transmitted information symbol by S_1. The received signal at D_1 and R can be respectively given by

$$y_{D_1}(k) = \mathbf{h}_{S_1 D_1}^H(k) \mathbf{w} x_{S_1}(k) + n(k) \tag{3.2}$$

and

$$y_R(k) = \mathbf{h}_{S_1 R}^H(k) \mathbf{w} x_{S_1}(k) + n(k), \tag{3.3}$$

where $\mathbf{h}_{S_1D_1}, \mathbf{h}_{S_1R} \in \mathbb{C}^{N\times 1}$. $\mathbf{w} \in \mathbb{C}^{N\times 1}$ represents the energy beamforming vector. As a result, the achievable information rate at D_1 can be given by

$$R_{S_1}^{(1)} = \tau_1 \mathcal{C}\left(\frac{|\mathbf{h}_{S_1D_1}^H \mathbf{w}|^2}{N_0}\right), \tag{3.4}$$

where $\mathcal{C}(x) \triangleq \log_2(1+x)$ and the harvested energy at R is

$$E_R = \eta\tau_1 |\mathbf{h}_{S_1R}^H \mathbf{w}|^2, \tag{3.5}$$

where $\eta \in [0,1]$ is a constant, accounting for the energy conversion efficiency. The larger the value of η, the higher the energy conversion efficiency. In particular, $\eta = 1$ means all received signal power can be perfectly converted to energy at the receiver. If we denote the transmit power at S_1 in the first phase to be $P_{S_1}^{(1)}$, it could be inferred that

$$\|\mathbf{w}\|^2 \leq P_{S_1}^{(1)}. \tag{3.6}$$

In the second phase, S_2 broadcasts information to R and D_2. Let the transmitted symbol by S_2 be $x_{S_2}(k)$. The signal received at R and D_2 can be respectively given by

$$y_R(k) = \sqrt{P_{S_2}^{(2)}} h_{S_2R}(k) x_{S_2}(k) + n(k) \tag{3.7}$$

and

$$y_{D_2}(k) = \sqrt{P_{S_2}^{(2)}} h_{S_2D_2}(k) x_{S_2}(k) + n(k), \tag{3.8}$$

where $P_{S_2}^{(2)}$ is the available transmit power at S_2 in the second phase.

In the third phase, R decode the information transmitted from S_2 and then help to forward the decoded information to D_2 by using the harvested energy from

S_1 in the first phase. The received signal at D_2 from R is

$$y_{D_2}(k) = \sqrt{P_R} h_{RD_2}(k) x_R(k) + n(k), \tag{3.9}$$

where P_R is the available transmit power at R in the third phase. As the available power at R must be constrained by E_R in (3.5), i.e., $P_R \leq \frac{E_R}{\tau_3}$, so we have that

$$\tau_3 P_R \leq \eta \tau_1 |\mathbf{h}_{S_1R}^H \mathbf{w}|^2. \tag{3.10}$$

Decode-and-forward (DF) relaying operation is employed at R, so the end-to-end achievable information of group 2 can be given by [38]

$$R_{S_2} = \min \left\{ \tau_2 \mathcal{C} \left(\frac{P_{S_2}^{(2)} |h_{S_2R}|^2}{N_0} \right), \tau_2 \mathcal{C} \left(\frac{P_{S_2}^{(2)} |h_{S_2D_2}|^2}{N_0} \right) + \tau_3 \mathcal{C} \left(\frac{P_R |h_{RD_2}|^2}{N_0} \right) \right\}. \tag{3.11}$$

In the fourth phase, S_1 transmits information to its destination D_1 via multiple antennas. As it is a typical multiple input single output (MISO) channel, the achievable information rate from S_1 to D_1 in this phase is [41]

$$R_{S_1}^{(4)} = \tau_4 \mathcal{C} \left(\frac{P_{S_1}^{(4)} \|\mathbf{h}_{S_1D_1}\|^2}{N_0} \right), \tag{3.12}$$

where $P_{S_1}^{(4)}$ is the available transmit power at S_1 in the fourth phase.

For the four phases described above, group 1 transmits information in both the first and the fourth phases. Combine $R_{S_1}^{(1)}$ with $R_{S_1}^{(4)}$, the total achievable information rate for S_1 in the k-th fading block is

$$R_{S_1} = R_{S_1}^{(1)} + R_{S_1}^{(4)} = \tau_1 \mathcal{C} \left(\frac{|\mathbf{h}_{S_1D_1}^H \mathbf{w}|^2}{N_0} \right) + \tau_4 \mathcal{C} \left(\frac{P_{S_1}^{(4)} \|\mathbf{h}_{S_1D_1}\|^2}{N_0} \right). \tag{3.13}$$

Group 2 transmits information in the second and the third phases via cooperative relaying, whose available information rate in the k-th fading block is shown in (3.11).

Besides, group 1 transmits energy to group 2 in the first phase and group 2 gives its bandwidth for the information transmission to group 1 in the first and fourth phases.

For such a system described above, we shall explore its performance limits in terms of WSR for given available power at S_1 and S_2 and the overall consumed power for given predefined information rate thresholds of the two groups. To this end, we consider the optimal design of the system by maximizing WSR and minimizing its total consumed power in Chapter 4 and Chapter 5.

Chapter 4: Weighted Sum Rate Maximization Design

In this section, we consider the minimal rate constrained weighted sum rate maximization design of the system. The goal is to explore the performance limit in terms of total achievable information rate with user's fairness. Different from existing WSR maximization in various wireless systems, where the minimal rate requirements of the users are not considered, in our work the minimal required rate can be guaranteed for each user.

Suppose the minimal required information rate of group i is r_{S_i}, where $i \in \{1, 2\}$. The end-to-end achievable information rate R_{S_i} satisfies that

$$R_{S_i} \geq r_{S_i}, \ \forall i = 1, 2. \tag{4.1}$$

With the minimal rate constraints in (4.1), the WSR of the system shall be maximized. Let α_i be the weight of achievable information rate of group i. The WSR of the system can be given by

$$R_{wsum} = \sum_{i=1}^{2} \alpha_i R_{S_i}. \tag{4.2}$$

. Actually, $\alpha_i \geq 0$ reflects the relative importance of group i.

Besides the minimal rate constraints, the available power at S_1 and S_2 should also be considered. In our work, we discuss two scenarios. In the first scenario,

S_1 transmits energy and information in the first and the fourth phases with the same fixed power, while in the second scenario, the consumed power in the first and fourth phases at S_1 is constrained by a given average power. The two scenarios are discussed in the following Section 4.1 and Section 4.2, respectively.

4.1 Fixed Power Constrained Scenario

4.1.1 Problem Formulation

In the fixed power scenario, S_1 and S_2 has fixed instantaneous power in their respective transmission phases, i.e., $P_{S_1}^{(1)} = P_{S_1}^{(4)}$. For convenience, we denote the fixed power at S_i to be P_{S_i}, so $P_{S_1}^{(1)} = P_{S_1}^{(4)} = P_{S_1}$ and $P_{S_2}^{(2)} = P_{S_2}$. As a result, (3.6), (3.11) and (3.13) can be respectively rewritten as

$$\|\mathbf{w}\|^2 \leq P_{S_1}, \tag{4.3}$$

$$R_{S_2} = \min\left\{\tau_2\mathcal{C}\left(\frac{P_{S_2}|h_{S_2R}|^2}{N_0}\right), \tau_2\mathcal{C}\left(\frac{P_{S_2}|h_{S_2D_2}|^2}{N_0}\right) + \tau_3\mathcal{C}\left(\frac{P_R|h_{RD_2}|^2}{N_0}\right)\right\}, \tag{4.4}$$

and

$$R_{S_1} = \tau_1\mathcal{C}\left(\frac{|\mathbf{h}_{S_1D_1}^H\mathbf{w}|^2}{N_0}\right) + \tau_4\mathcal{C}\left(\frac{P_{S_1}\|\mathbf{h}_{S_1D_1}\|^2}{N_0}\right). \tag{4.5}$$

Therefore, the WSR maximization problem for fixed power scenario can be mathematically expressed as

$$\begin{aligned} \mathbf{P}_1: \underset{\boldsymbol{\tau},\mathbf{w}}{\text{maximize}} \quad & \alpha_1 R_{S_1} + \alpha_2 R_{S_2} \\ \text{subject to} \quad & (3.1), (3.10), \\ & (4.1), (4.3), (4.4), (4.5). \end{aligned}$$

It can be observed that the right sides of (4.4) and (4.5) are non-linear w.r.t. $\boldsymbol{\tau}$ and $\mathbf{w}$, so constraints (4.4) and (4.5) are non-convex sets. Moreover, (3.10) and (4.1) are also non-convex sets w.r.t. $\boldsymbol{\tau}$ and $\mathbf{w}$. Therefore, $\mathbf{P}_1$ is not a convex problem and cannot be solved with known solution methods. Thus, we solve it as follows.

4.1.2 Problem Transformation and Solution

We observe that $\mathbf{w}$ always appears in a quadratic form as shown in constraints (3.10), (4.3) and (4.5). By defining $\mathbf{W} \triangleq \mathbf{w}\mathbf{w}^H$, the three constraints mentioned above can be reinterpreted as

$$\tau_3 P_R \leq \eta \tau_1 \mathbf{h}_{S_1R}^H \mathbf{W} \mathbf{h}_{S_1R}, \tag{4.6}$$

$$\mathrm{Tr}(\mathbf{W}) \leq P_{S_1}, \tag{4.7}$$

and

$$R_{S_1} = \tau_1 \mathcal{C}\left(\frac{\mathbf{h}_{S_1D_1}^H \mathbf{W} \mathbf{h}_{S_1D_1}}{N_0}\right) + \tau_4 \mathcal{C}\left(\frac{P_{S_1}\|\mathbf{h}_{S_1D_1}\|^2}{N_0}\right). \tag{4.8}$$

Note that in order to ensure that $\mathbf{w}$ could be recovered by $\mathbf{W}$ uniquely, it must satisfy that

$$\mathbf{W} \succeq 0, \tag{4.9}$$

and

$$\mathrm{rank}(\mathbf{W}) = 1. \tag{4.10}$$

Therefore, by replacing $\mathbf{w}$ with $\mathbf{W}$, problem $\mathbf{P}_1$ is equivalently transformed

into the following problem $\mathbf{P}_1'$,

$$\begin{aligned}\mathbf{P}_1': \underset{\boldsymbol{\tau},\mathbf{W}}{\text{maximize}} \quad & \alpha_1 R_{S_1} + \alpha_2 R_{S_2} \\ \text{subject to} \quad & (3.1), (4.1), (4.4), (4.6), \\ & (4.7), (4.8), (4.9), (4.10).\end{aligned}$$

It can be seen that $\mathbf{P}_1'$ is still not jointly convex w.r.t. $\boldsymbol{\tau}$ and $\mathbf{W}$ even though the rank-one constraint (4.10) is removed. However, it can be observed that when the rank-one constraint is dropped, for a given $\boldsymbol{\tau}$, it is convex w.r.t. $\mathbf{W}$. Meanwhile, for a given $\mathbf{W}$, it is convex w.r.t. $\boldsymbol{\tau}$. Therefore, the relaxed problem of $\mathbf{P}_1'$ can be solved by using traditional alternative iteration solution method. Nevertheless, with the traditional solution method, it cannot be theoretically proved that the global optimal solution can always be guaranteed.

In order to pursue the global optimum, we design a new solution method as follows which is capable of finding the global optimal solution for Problem $\mathbf{P}_1'$.

Define a new matrix variable $\mathbf{V} \in \mathbb{C}^{N\times N}$ such that $\mathbf{V} = \tau_1 \mathbf{W}$. Since (4.9) and (4.10), it is known that,

$$\mathbf{V} \succeq 0, \tag{4.11}$$

and

$$\text{rank}(\mathbf{V}) = 1. \tag{4.12}$$

By substitution of $\mathbf{V}$ into (4.7) and (4.8), the two constraints can be re-expressed by

$$\text{Tr}(\mathbf{V}) \leq \tau_1 P_{S_1}, \tag{4.13}$$

and

$$R_{S_1} = \tau_1 \mathcal{C}\left(\frac{\mathrm{Tr}(\mathbf{V}\mathbf{h}_{S_1D_1}\mathbf{h}_{S_1D_1}^H)}{N_0\tau_1}\right) + \tau_4 \mathcal{C}\left(\frac{P_{S_1}\|\mathbf{h}_{S_1D_1}\|^2}{N_0}\right), \tag{4.14}$$

respectively.

Moreover, let $\phi_1 = \tau_3 P_R$. (4.6) and (4.4) can be respectively rewritten as

$$\phi_1 \leq \eta \mathrm{Tr}(\mathbf{V}\mathbf{h}_{S_1R}\mathbf{h}_{S_1R}^H) \tag{4.15}$$

and

$$R_{S_2} = \min\left\{\tau_2 \mathcal{C}\left(\frac{P_{S_2}|h_{S_2R}|^2}{N_0}\right), \tau_2 \mathcal{C}\left(\frac{P_{S_2}|h_{S_2D_2}|^2}{N_0}\right) + \tau_3 \mathcal{C}\left(\frac{\phi_1|h_{RD_2}|^2}{N_0\tau_3}\right)\right\}. \tag{4.16}$$

With above variable substitution operations, i.e., $\mathbf{V} = \tau_1\mathbf{W}, \phi_1 = \tau_3 P_R$, Problem $\mathbf{P}_1'$ is equivalently transformed into the following Problem $\mathbf{P}_1''$,

$$\begin{aligned} \mathbf{P}_1'': \underset{\boldsymbol{\tau},\mathbf{V},\phi_1}{\text{maximize}} \quad & \alpha_1 R_{S_1} + \alpha_2 R_{S_2} \\ \text{subject to} \quad & (3.1), (4.1), (4.11), (4.12), \\ & (4.13), (4.14), (4.15), (4.4). \end{aligned}$$

It can be seen that the objective function of Problem $\mathbf{P}_1''$ is a concave function. All constraints except rank-one constraint (4.12) are convex sets. So we may get rid of (4.12) and make the problem to be convex by using Semi-definite Relaxation (SDR) [44], i.e.,

$$\begin{aligned} \mathbf{P}_1''': \underset{\boldsymbol{\tau},\mathbf{V},\phi_1}{\text{minimize}} \quad & -\alpha_1 R_{S_1} - \alpha_2 R_{S_2} \\ \text{subject to} \quad & (3.1), (3.11), (4.1), (4.11), \\ & (4.13), (4.14), (4.15), \end{aligned}$$

which is in a standard form of convex problem and the optimal $[\boldsymbol{\tau}^*, \mathbf{V}^*, \phi_1^*]$ of Problem $\mathbf{P}_1'''$ can be obtained by using some known solution methods, e.g., interior point method, for convex problems [43].

Note that only when $\text{rank}(\mathbf{V}^*) = 1$, $[\boldsymbol{\tau}^*, \mathbf{V}^*, \phi_1^*]$ is also the optimal solution of Problem $\mathbf{P}_1''$. In this case, the optimal $[\boldsymbol{\tau}^*, \mathbf{w}^*]$ can be derived accordingly. Therefore, the key question lies in the rank of $\mathbf{V}^*$. Fortunately, we found that there exists an optimal $\mathbf{V}^*$ such that $\text{rank}(\mathbf{V}^*) = 1$ for Problem $\mathbf{P}_1'''$, which means the global optimum of the primary Problem $\mathbf{P}_1$ can be guaranteed.

Now we analyse the rank of $\mathbf{V}^*$ with Theorem 4.1. Before that, we present Lemma 4.1 which was proved in [42] for emphasis as follows.

Lemma 4.1. *[42] Consider a problem* $\mathbf{P}_0$,

$$\begin{aligned} \mathbf{P}_0 : \underset{\mathbf{X}_1,\ldots,\mathbf{X}_L}{\textit{minimize}} \quad & \sum_{l=1}^{L} Tr(\mathbf{C}_l\mathbf{X}_l) \\ \textit{subject to} \quad & \sum_{l=1}^{L} Tr(\mathbf{A}_{ml}\mathbf{X}_l) \trianglerighteq_m b_m,\ m = 1,\ldots,M, \\ & \mathbf{X}_l \succeq 0,\ l = 1,\ldots,L, \end{aligned}$$

where $\mathbf{C}_l, l = 1,\ldots,L$ *and* $\mathbf{A}_{ml}, m = 1,\ldots,M, l = 1,\ldots,L$ *are Hermitian matrices,* $b \in \mathbb{R}$, $\trianglerighteq_m \in \{\geq, =, \leq\}, m = 1,\ldots,M$ *and the variables* $\mathbf{X}_l, l = 1,\ldots,L$ *are Hermitian matrices.*

If Problem $\mathbf{P}_0$ *and its dual are solvable, then the Problem* $\mathbf{P}_0$ *has always an optimal solution* $(\mathbf{X}_1^*,\ldots,\mathbf{X}_L^*)$ *such that*

$$\sum_{l=1}^{L} rank^2(\mathbf{X}_l^*) \leq M.$$

Theorem 4.1. *There exists an optimal* $\mathbf{V}^*$ *of Problem* $\mathbf{P}_1'''$ *such that rank*$(\mathbf{V}^*) = 1$.

Proof. First, we consider the following Problem $\mathbf{Q}_1$,

$$\begin{aligned}
\mathbf{Q}_1: \underset{\mathbf{U}}{\text{minimize}} \quad & \text{Tr}(\mathbf{U}) \\
\text{subject to} \quad & \phi_1^* \leq \eta \text{Tr}(\mathbf{U}\mathbf{h}_{S_1R}\mathbf{h}_{S_1R}^H), \\
& R_{S_1}^* = \tau_1^* \mathcal{C}\left(\frac{\text{Tr}(\mathbf{U}\mathbf{h}_{S_1D_1}\mathbf{h}_{S_1D_1}^H)}{N_0\tau_1^*}\right) + \tau_4^* \mathcal{C}\left(\frac{P_{S_1}\|\mathbf{h}_{S_1D_1}\|^2}{N_0}\right), \\
& \mathbf{U} \succeq 0,
\end{aligned}$$

where τ_1^*, τ_4^*, $\phi_1^*$and $R_{S_1}^*$ are optimal solutions of Problem $\mathbf{P}_1'''$. Problem $\mathbf{Q}_1$ is equivalently transformed into Problem $\mathbf{Q}_1'$,

$$\begin{aligned}
\mathbf{Q}_1': \underset{\mathbf{U}}{\text{minimize}} \quad & \text{Tr}(\mathbf{U}) \\
\text{subject to} \quad & \text{Tr}(\mathbf{U}\mathbf{h}_{S_1R}\mathbf{h}_{S_1R}^H) \geq \frac{\phi_1^*}{\eta}, \\
& \text{Tr}(\mathbf{U}\mathbf{h}_{S_1D_1}\mathbf{h}_{S_1D_1}^H) = N_0\tau_1^* \left(2^{\frac{R_{S_1}^* - \tau_4^* \mathcal{C}\left(\frac{P_{S_1}\|\mathbf{h}_{S_1D_1}\|^2}{N_0}\right)}{\tau_1^*}} - 1\right), \\
& \mathbf{U} \succeq 0,
\end{aligned}$$

According to Lemma 4.1, Problem $\mathbf{Q}_1$ has an optimal solution $\mathbf{U}^*$ which satisfies that

$$\text{rank}^2(\mathbf{U}^*) \leq 2.$$

Moreover, since $\text{rank}(\mathbf{U}^*) \neq 0$, we conclude that $\text{rank}(\mathbf{U}^*) = 1$.

Let $[\boldsymbol{\tau}^*, \mathbf{V}^*, \phi_1^*]$ be the optimal solution of Problem $\mathbf{P}_1'''$. It can be inferred that $\mathbf{V}^*$ is a feasible solution of Problem $\mathbf{Q}_1$. The reason is that $[\boldsymbol{\tau}^*, \mathbf{V}^*, \phi_1^*]$ also satisfy the constraints (4.14) and (4.15). The optimal value of Problem $\mathbf{Q}_1$ associated with $\mathbf{U}^*$ must be smaller than that associated with any other feasible solution. Therefore, $\text{Tr}(\mathbf{U}^*) \leq \text{Tr}(\mathbf{V}^*) \leq \tau_1^* P_{S_1}$.

If we construct a new tuple $[\boldsymbol{\tau}^*, \mathbf{U}^*, \phi_1^*]$, then it satisfy all constraints of Problem $\mathbf{P}_1'''$, which means it is a feasible solution of Problem $\mathbf{P}_1'''$. Since the objective function of Problem $\mathbf{P}_1'''$ is only related to $\boldsymbol{\tau}$ and ϕ_1, $[\boldsymbol{\tau}^*, \mathbf{U}^*, \phi_1^*]$ and $[\boldsymbol{\tau}^*, \mathbf{V}^*, \phi_1^*]$ yield the same value of Problem $\mathbf{P}_1'''$, which means that $[\boldsymbol{\tau}^*, \mathbf{U}^*, \phi_1^*]$ is also an optimal solution of Problem $\mathbf{P}_1'''$. Since we have proved that $\text{rank}(\mathbf{U}^*) = 1$, it can be concluded that $\mathbf{P}_1'''$ has an optimal rank-one solution. □

Remark 4.1. *The optimal solution of Problem* $\mathbf{P}_1$ *for the fixed power scenario is guaranteed to be found.*

The reason for Remark 4.1 is explained as follows. $\mathbf{P}_1$, $\mathbf{P}_1'$ and $\mathbf{P}_1''$ are equivalent to each other. It is known that once the optimal solution of $\mathbf{P}_1'''$ satisfies the rank-one constraint, it is equivalent to $\mathbf{P}_1$, $\mathbf{P}_1'$ and $\mathbf{P}_1''$. Theorem 4.1 declares that $\mathbf{P}_1'''$ has a rank-one optimal solution. Therefore, the optimal solution for Problem $\mathbf{P}_1$ can always be found by using our proposed solution method.

4.2 Average Power Constrained Scenario

4.2.1 Problem Formulation

In this scenario, S_1 and S_2 are allowed to transmit information/energy in different phases with different power, but the averaged power over each fading block is limited by P_{S_1} and P_{S_2} respectively. That is, the consumed power at S_1 and S_2 satisfy that

$$\tau_1 P_{S_1}^{(1)} + \tau_4 P_{S_1}^{(4)} \leq P_{S_1}, \tag{4.17}$$

and

$$\tau_2 P_{S_2}^{(2)} \leq P_{S_2}. \tag{4.18}$$

For clarity, we define $\mathbf{P} \triangleq [P_{S_1}^{(1)} \ P_{S_1}^{(4)} \ P_{S_2}^{(2)}]^T$. Therefore, the WSR maximization problem can be mathematically expressed by

$$\begin{aligned} \mathbf{P}_2 : \underset{\boldsymbol{\tau},\mathbf{w},\mathbf{P}}{\text{maximize}} \quad & \alpha_1 R_{S_1} + \alpha_2 R_{S_2} \\ \text{subject to} \quad & (3.1), (3.6), (3.11), (3.10), \\ & (3.13), (4.1), (4.17), (4.18). \end{aligned}$$

Compared with Problem $\mathbf{P}_1$ for the fixed power constrained scenario, in Problem $\mathbf{P}_2$, the power $\mathbf{P}$ consumed in each phase at the two sources are also optimized besides $\boldsymbol{\tau}$ and $\mathbf{w}$. It can be observed that Problem $\mathbf{P}_2$ is also non-convex. So we solve it as follows.

4.2.2 Problem Transformation and Solution

Similar to the solution method designed for Problem $\mathbf{P}_1$, we also deal with Problem $\mathbf{P}_2$ by transforming it to a convex problem through variable substitution operations and SDR method at first and then solve it efficiently.

We also use the definition of $\mathbf{W} = \mathbf{w}\mathbf{w}^H$ by introducing a semi-definite square matrix $\mathbf{W}$, i.e., $\mathbf{W} \succeq 0$. Then, (3.10) can be equivalently replaced by (4.6) and constraints (3.6) and (3.13) can be respectively re-expressed by

$$\mathrm{Tr}(\mathbf{W}) \leq P_{S_1}^{(1)}, \tag{4.19}$$

and

$$R_{S_1} = \tau_1 \mathcal{C}\left(\frac{\mathbf{h}_{S_1D_1}^H \mathbf{W} \mathbf{h}_{S_1D_1}}{N_0}\right) + \tau_4 \mathcal{C}\left(\frac{P_{S_1}^{(4)} \|\mathbf{h}_{S_1D_1}\|^2}{N_0}\right). \tag{4.20}$$

Consequently, with the rank-one constraint of $\mathbf{W}$, i.e., $\text{rank}(\mathbf{W}) = 1$, Problem $\mathbf{P}_2$ is equivalently transformed into the following Problem $\mathbf{P}_2'$, i.e.,

$$\begin{aligned}\mathbf{P}_2': \underset{\boldsymbol{\tau},\mathbf{W},\mathbf{P}}{\text{maximize}} \quad & \alpha_1 R_{S_2} + \alpha_2 R_{S_1} \\ \text{subject to} \quad & (3.1), (3.11), (4.1), (4.6), (4.9), \\ & (4.10), (4.17), (4.18), (4.19), (4.20).\end{aligned}$$

Since Problem $\mathbf{P}_2'$ is still non-convex, we further adopt the following variable substitutions by introducing five new variables, i.e.,

$$\begin{cases} \mathbf{V} = & \tau_1 \mathbf{W}, \\ \phi_1 = & \tau_3 P_R, \\ \phi_2 = & \tau_2 P_{S_2}^{(2)}, \\ \phi_3 = & \tau_1 P_{S_1}^{(1)}, \\ \phi_4 = & \tau_4 P_{S_1}^{(4)}. \end{cases} \tag{4.21}$$

With these linear definitions, (4.6), (4.9) and (4.10) can be replaced by (4.15), (4.11) and (4.12). Besides, (3.11), (4.17), (4.18), (4.19) and (4.20) are respectively transformed into

$$R_{S_2} = \min\left\{\tau_2 \mathcal{C}\left(\frac{\phi_2 |h_{S_2 R}|^2}{N_0 \tau_2}\right), \tau_2 \mathcal{C}\left(\frac{\phi_2 |h_{S_2 D_2}|^2}{N_0 \tau_2}\right) + \tau_3 \mathcal{C}\left(\frac{\phi_1 |h_{R D_2}|^2}{N_0 \tau_3}\right)\right\}, \tag{4.22}$$

$$\phi_3 + \phi_4 \leq P_{S_1}, \tag{4.23}$$

$$\phi_2 \leq P_{S_2}, \tag{4.24}$$

$$\text{Tr}(\mathbf{V}) \leq \phi_3 \tag{4.25}$$

and

$$R_{S_1} = \tau_1 \mathcal{C}\left(\frac{\mathrm{Tr}(\mathbf{V}\mathbf{h}_{S_1D_1}\mathbf{h}_{S_1D_1}^H)}{N_0\tau_1}\right) + \tau_4 \mathcal{C}\left(\frac{\phi_4\|\mathbf{h}_{S_1D_1}\|^2}{N_0\tau_4}\right). \tag{4.26}$$

Define $\boldsymbol{\phi} = [\phi_1\ \phi_2\ \phi_3\ \phi_4]^T$. Therefore, Problem $\mathbf{P}_2'$ can be equivalently transformed into the following Problem $\mathbf{P}_2''$,

$$\begin{aligned} \mathbf{P}_2'' : \underset{\boldsymbol{\tau},\mathbf{V},\boldsymbol{\phi}}{\text{maximize}} \quad & \alpha_1 R_{S_2} + \alpha_2 R_{S_1} \\ \text{subject to} \quad & (3.1), (4.1), (4.11), (4.12), (4.15), \\ & (4.22), (4.23), (4.24), (4.25), (4.26). \end{aligned}$$

It can be seen that the objective function of Problem $\mathbf{P}_2''$ is concave and all constraints except the rank-one constraint (4.12) are convex sets. Therefore, by using SDR method with the dropping of (4.12), Problem $\mathbf{P}_2''$ can be relaxed to a convex problem as follows,

$$\begin{aligned} \mathbf{P}_2''' : \underset{\boldsymbol{\tau},\mathbf{V},\boldsymbol{\phi}}{\text{minimize}} \quad & -\alpha_1 R_{S_1} - \alpha_2 R_{S_2} \\ \text{subject to} \quad & (3.1), (3.11), (4.1), (4.11), (4.15), \\ & (4.22), (4.23), (4.24), (4.25), (4.26). \end{aligned}$$

Therefore, the optimal solution $[\boldsymbol{\tau}^*, \mathbf{V}^*, \boldsymbol{\phi}^*]$ of Problem $\mathbf{P}_2'''$ can be obtained by using some known solution methods.

Similar to the situation of Problem $\mathbf{P}_1'''$, only when $\mathrm{rank}(\mathbf{V}^*) = 1$, $[\boldsymbol{\tau}^*, \mathbf{V}^*, \boldsymbol{\phi}^*]$ is also the optimal solution of Problem $\mathbf{P}_2''$. In this case, the optimal $[\boldsymbol{\tau}^*, \mathbf{w}^*, \mathbf{P}^*]$ can be derived accordingly. Therefore, the key question lies in the rank of $\mathbf{V}^*$. Fortunately, we also found that $\mathrm{rank}(\mathbf{V}^*) = 1$ always holds for Problem $\mathbf{P}_2'''$, which means the global optimum of the primary Problem $\mathbf{P}_2$ also can be guaranteed by our adopted variable substitutions and SDR.

Now we analyse the rank of $\mathbf{V}^*$ for the average power constrained scenario with Theorem 4.2.

Theorem 4.2. *There exists an optimal* $\mathbf{V}^*$ *of Problem* $\mathbf{P}_2'''$ *such that rank*$(\mathbf{V}^*) = 1$.

Proof. First, we consider the following Problem $\mathbf{Q}_2$,

$$\begin{aligned}
\mathbf{Q}_2 : \underset{\mathbf{U}}{\text{minimize}} \quad & \text{Tr}(\mathbf{U}) \\
\text{subject to} \quad & \phi_1^* \leq \eta \text{Tr}(\mathbf{U}\mathbf{h}_{S_1R}\mathbf{h}_{S_1R}^H), \\
& R_{S_1}^* = \tau_1^* \mathcal{C}\left(\frac{\text{Tr}(\mathbf{U}\mathbf{h}_{S_1D_1}\mathbf{h}_{S_1D_1}^H)}{N_0\tau_1^*}\right) + \tau_4^* \mathcal{C}\left(\frac{\phi_4^* \|\mathbf{h}_{S_1D_1}\|^2}{N_0\tau_4^*}\right), \\
& \mathbf{U} \succeq 0,
\end{aligned}$$

where τ_1^*, τ_4^*, ϕ_1^*, ϕ_4^* and $R_{S_1}^*$ are optimal solutions of Problem $\mathbf{P}_2'''$. Problem $\mathbf{Q}_2$ is equivalently transformed into Problem $\mathbf{Q}_2'$,

$$\begin{aligned}
\mathbf{Q}_2' : \underset{\mathbf{U}}{\text{minimize}} \quad & \text{Tr}(\mathbf{U}) \\
\text{subject to} \quad & \text{Tr}(\mathbf{U}\mathbf{h}_{S_1R}\mathbf{h}_{S_1R}^H) \geq \frac{\phi_1^*}{\eta}, \\
& \text{Tr}(\mathbf{U}\mathbf{h}_{S_1D_1}\mathbf{h}_{S_1D_1}^H) = N_0\tau_1^* \left(2^{\frac{R_{S_1}^* - \tau_4^* \mathcal{C}\left(\frac{\phi_4^* \|\mathbf{h}_{S_1D_1}\|^2}{N_0\tau_4^*}\right)}{\tau_1^*}} - 1\right), \\
& \mathbf{U} \succeq 0,
\end{aligned}$$

According to Lemma 4.1, Problem $\mathbf{Q}_2$ has an optimal solution $\mathbf{U}^*$ which satisfies that

$$\text{rank}^2(\mathbf{U}^*) \leq 2.$$

Since $\text{rank}(\mathbf{U}^*) \neq 0$, we conclude that $\text{rank}(\mathbf{U}^*) = 1$.

Let $[\boldsymbol{\tau}^*, \mathbf{V}^*, \boldsymbol{\phi}^*]$ be the optimal solution of Problem $\mathbf{P}_2'''$. It can be inferred that $\mathbf{V}^*$ is a feasible solution of Problem $\mathbf{Q}_2$. The reason is that $[\boldsymbol{\tau}^*, \mathbf{V}^*, \boldsymbol{\phi}^*]$ also satisfy

the constraints (4.15) and (4.26). The optimal value of Problem $\mathbf{Q}_2$ associated with $\mathbf{U}^*$ must be smaller than that associated with any other feasible solution. Therefore, $\mathrm{Tr}(\mathbf{U}^*) \leq \mathrm{Tr}(\mathbf{V}^*) \leq \phi_3^*$.

If we construct a new tuple $[\boldsymbol{\tau}^*, \mathbf{U}^*, \boldsymbol{\phi}^*]$, then it satisfy all constraints of Problem $\mathbf{P}_2'''$, which means it is a feasible solution of Problem $\mathbf{P}_2'''$. Since the objective function of Problem $\mathbf{P}_2'''$ is only related to $\boldsymbol{\tau}$ and $\boldsymbol{\phi}$, $[\boldsymbol{\tau}^*, \mathbf{U}^*, \boldsymbol{\phi}^*]$ and $[\boldsymbol{\tau}^*, \mathbf{V}^*, \boldsymbol{\phi}^*]$ yield the same value of Problem $\mathbf{P}_2'''$, which means that $[\boldsymbol{\tau}^*, \mathbf{U}^*, \boldsymbol{\phi}^*]$ is also an optimal solution of Problem $\mathbf{P}_2'''$. Since we have proved that $\mathrm{rank}(\mathbf{U}^*) = 1$, we conclude that $\mathbf{P}_2'''$ has an optimal rank-one solution. □

Remark 4.2. *The optimal solution of Problem* $\mathbf{P}_2$ *for the average power constrained scenario is guaranteed to be found.*

The reason for Remark 4.2 is explained as follows. $\mathbf{P}_2$, $\mathbf{P}_2'$ and $\mathbf{P}_2''$ are equivalent to each other. It is known that once the optimal solution of $\mathbf{P}_2'''$ satisfies the rank-one constraint, it is equivalent to $\mathbf{P}_2$, $\mathbf{P}_2'$ and $\mathbf{P}_2''$. Theorem 4.2 declares that $\mathbf{P}_2'''$ has a rank-one optimal solution. Therefore, the optimal solution for Problem $\mathbf{P}_2$ can always be found by using our proposed solution method.

4.3 Simulations and Discussion

In this section, we present some numerical results to show the system performance of the considered WPCN in terms of weighted sum rate. Both the fixed power scenario and the average power constrained scenario are simulated and discussed.

In the simulations, the noise power N_0 is set to -30dBm and the energy conver-

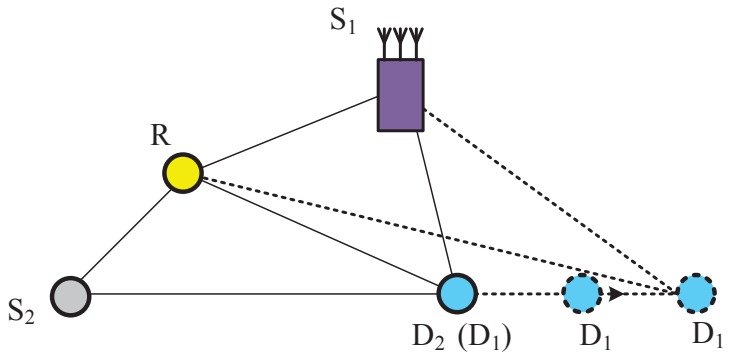

Figure 4.1: Simulation topology.

sion efficiency η is assumed to be 0.9. $h_{ij}(k) \sim \mathcal{CN}(0, d_{ij}^{-\alpha})$ is generated randomly and the path loss exponent factor α is set to 2. The considered network topology is shown in Figure 4.1, where $d_{S_1R} = 2m$, $d_{S_1D_1} = 9m$, $d_{S_2R} = 5m$, $d_{S_2D_2} = 12m$, $d_{RD_1} = d_{RD_2} = 10m$. The antenna number is set to 4. α_1 and α_2 are both equal to 1 so that total sum rate of the system is measured. P_{S_1} is 2 watts and P_{S_2} is 200 mW. The minimum required information rate r_{S_1} and r_{S_2} are set to be 1.4bit/s and 0.7bit/s, respectively. Unless otherwise specified, the above parameters will not be changed.

For comparison, two benchmark methods are also simulated. The first one is with equal time assignment method, where only beamforming vector $\mathbf{w}$ is optimized. That is, $\tau_1 = \tau_2 = \tau_3 = \tau_4 = 0.25$. The second is with random beamforming vector method, where only time assignment $\boldsymbol{\tau}$ is optimized and the beamforming vector $\mathbf{w}$ is randomly generated.

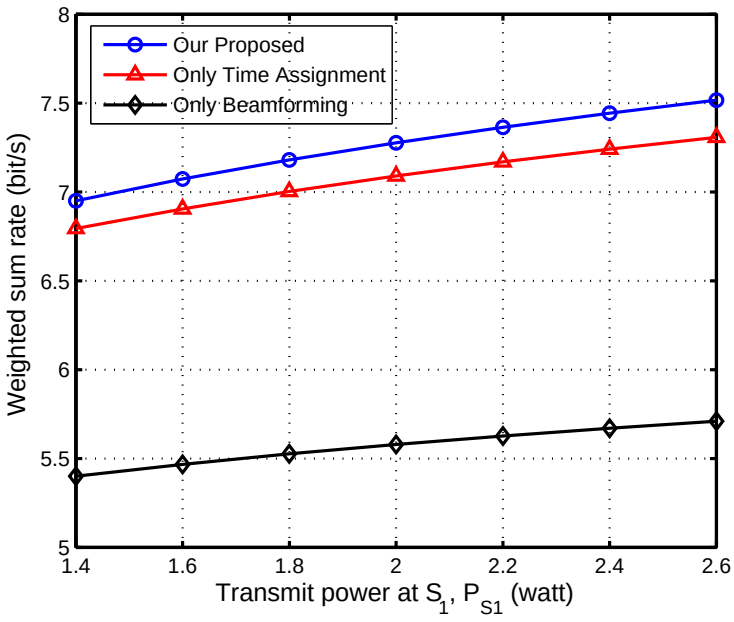

Figure 4.2: Weighted sum rate vs P_{S_1}.

4.3.1 Simulations for Fixed Power Scenario

In Figure 4.2, the WSR of the three schemes versus P_{S_1} are presented. It can be seen that, with the increment of P_{S_1}, the WSR of the fixed power scenario and those of the two benchmarks increase. The reason is straightforward, because more power will bring higher information rate. It also can be observed that the benchmark method which only involves the time assignment has much higher WSR than the benchmark which only involves beamforming. This indicates that in the considered WPCN system, the time assignment (also can be considered as bandwidth allocation) has greater impact on the system performance than the beamforming at S_1. The reason may be explained as follows. The beamforming design affects the system performance by energy transfer, which directly works on R and D_1. Since the power transfer over wireless channels is faded seriously, its effects is relatively

limited; while the time assignment works on all the transmits nodes and relay node, which adjust the system resources more systematically. Therefore, time assignment has much greater impact on system performance. It also indicates that for such kind of WPCNs, time assignment is more important in enhancing system performance.

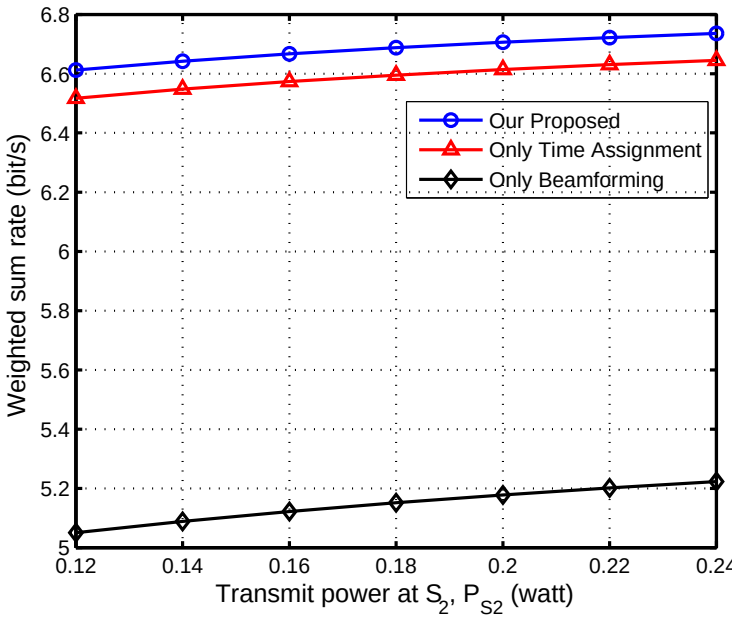

Figure 4.3: Weighted sum rate vs P_{S_2}.

Figure 4.3 plots the WSRs of the three schemes versus P_{S_2}. It also can be seen that with the increment of P_{S_2}, the system performances of the three methods also can be increased. Similar to Figure 4.2, it also can be observed that the time assignment plays more important role than the beamforming design in our considered WPCN system.

In order to get much deeper insignts, in Figure 4.4 and 4.5, the normalized performance gain versus P_{S_1} and P_{S_2} are respectively provided. In the two Figures, the WSRs of our proposed joint beamforming and time assignment method and the

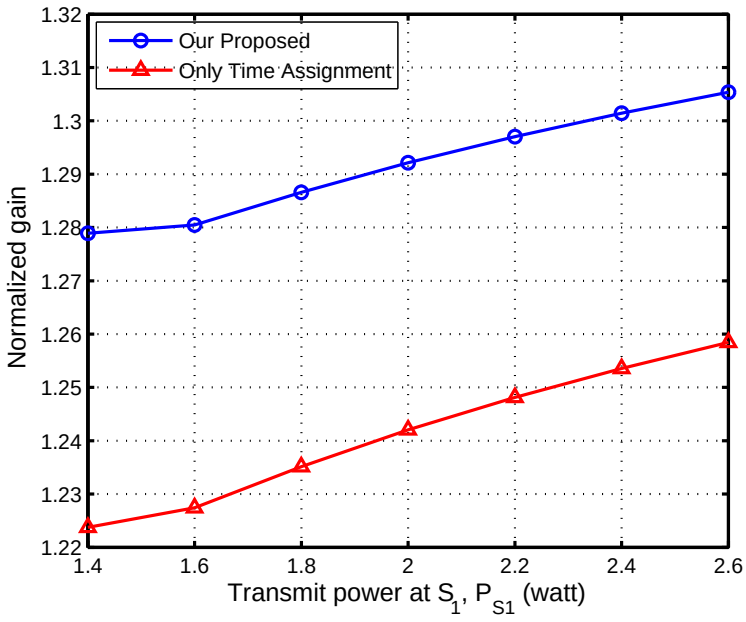

Figure 4.4: Normalized gain vs P_{S_1}.

benchmark method involving only time assignment are normalized (i.e., divided) by that of the benchmark method involving only beamforming. The higher of the ratio, the higher of the normalized performance gain. The two Figures show very different performance behavior of the system versus P_{S_1} and P_{S_2}. Specifically, in Figure 4.4, it shows that the normalized gains of our proposed scheme and the and the benchmark method involving only time assignment increase with the increment of P_{S_1}. While, in Figure 4.4, it shows that the normalized gains of our proposed scheme and the and the benchmark method involving only time assignment decrease with the increment of P_{S_2}. Moreover, it shows that in our numerical experiments, our proposed scheme is able to improve the system WSR at least 1.28 times that of the benchmark method involving only beamforming for a given P_{S_2} and improve the system weighted sum rate at most 1.3 times that of the benchmark method

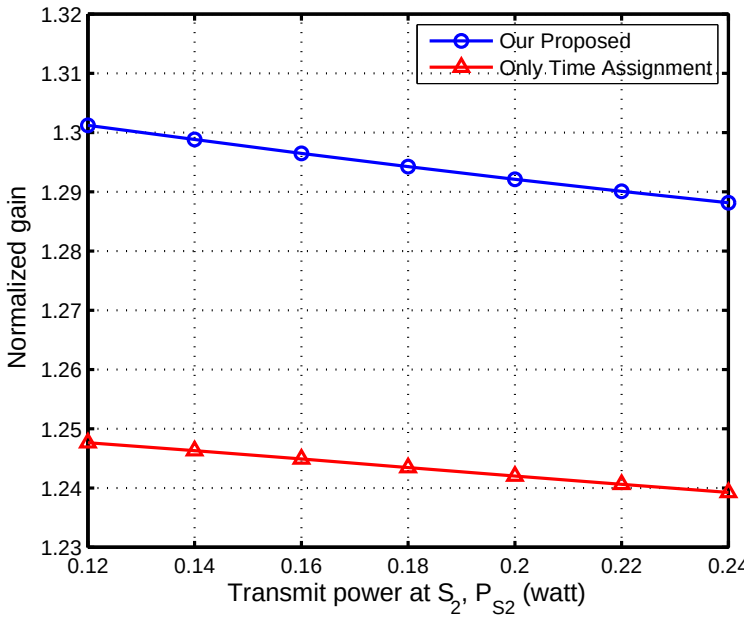

Figure 4.5: Normalized gain vs P_{S_2}.

involving only beamforming for a given P_{S_2}. This means that increasing either of P_{S_1} and P_{S_2} may enhance the system performance, but increasing P_{S_1} can bring much greater performance gain for the system.

In Figure 4.6, we simulate a dynamic scenario where D_1 moves away from S_1 along the line of $S_2 - D_2$ line, as shown in Figure 4.1. We desire to evaluate the impact of the distance $d_{S_1D_1}$ on system performance. It can be seen that with the increment of $d_{S_1D_1}$, the WSR is decreasing. However, the curve is getting flat, which means that if we further increase the distance $d_{S_1D_1}$, the service will not degrade too much. The reason may be that when $d_{S_1D_1}$ is relatively large, stronger signals should be transmitted by S_1 to D_1 to meet the minimal data rate requirement of D_1. This affects the beamforming weight and the time allocation of the system. That is, less power can be harvested by R and also to make the system performance

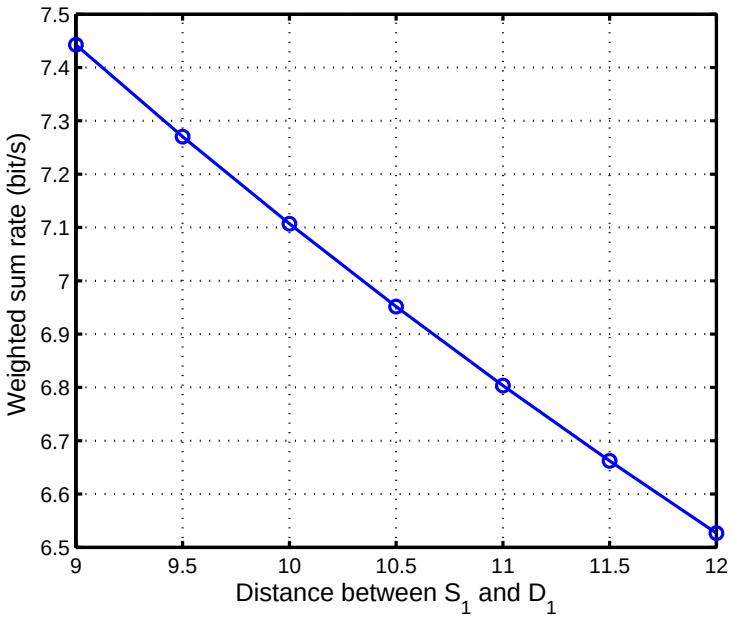

Figure 4.6: Weighted sum rate vs $d_{S_1D_1}$.

decrease as less as possible, the time interval of the first phase is increased and that of the fourth phase is decreased.

In Figure 4.7, the WSR is plotted versus the number of antennas of S_1. One can see that as antenna number increases, the system performance is also increasing. Moreover, it also shows that with the increment of the number of antennas, the increasing rate of the weighted sum rate roughly decreases, which means that increasing the number of antennas is able to enhance system performance, but it cannot increase the system performance infinitely.

Besides, the predefined weights of the achievable information rate of the two groups may also affect the total throughput of system. In Problem $\mathbf{P}_1$, when $\alpha_1 = \alpha_2$ and $r_{S_1} \neq 0$ and $r_{S_2} \neq 0$, it means that both groups have minimal required data rate and both of them have the same importance on the contribution to the system

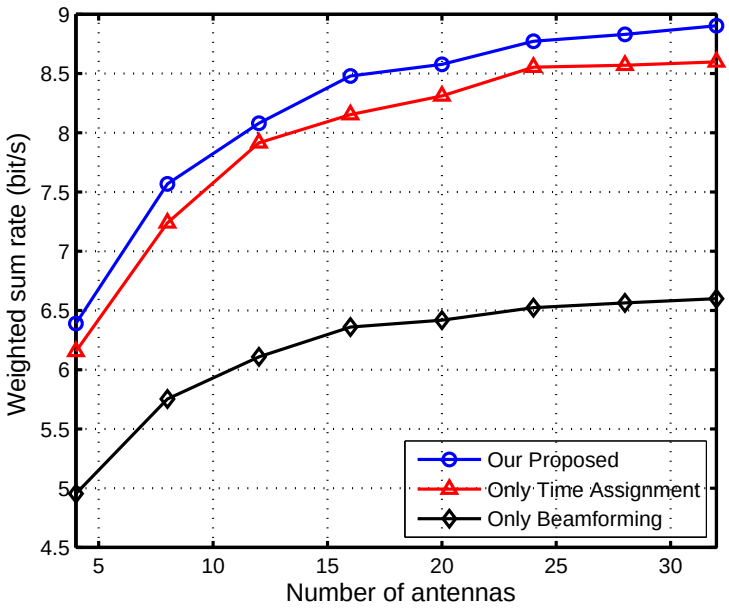

Figure 4.7: Weighted sum rate vs number of antennas.

total throughput. If we set $\alpha_1 = 0$, $r_{S_2} = 0$, it will arouse a new system design with new purpose, i.e., guaranteeing the minimal required data rate of the bandwidth-limited user pair (group 1) while maximizing the achievable information rate of the energy-limited user pair (group 2). Moreover, if we set $\alpha_2 = 0$, $r_{S_1} = 0$, it will arouse a system design with another new purpose, i.e., guaranteeing the minimal required data rate of the power-limited user pair (group 2) while maximizing the achievable information rate of the bandwidth-limited user pair (group 1). In these two configurations, the priorities or the importance of the two groups are very different, where only one group' communication quality can be guaranteed. Figure 4.8 and 4.9 provide some numerical results of the system performance associated with different α_1, α_2, r_{S_1} and r_{S_2} versus P_{S_1} and P_{S_2}, respectively. From the two Figures, it can be observed that the system with the configuration of $\alpha_1 = 1$, $\alpha_2 = 1$,

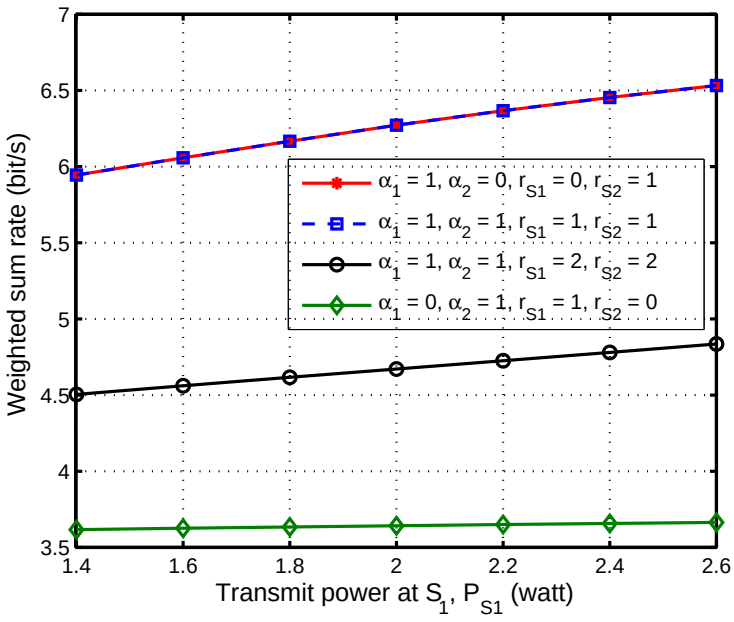

Figure 4.8: Weighted sum rate vs P_{S_1} for different α_1, α_2, r_{S_1} and r_{S_2}

$r_{S_1} = 1$ and $r_{S_2} = 1$ yields the highest system throughput among the four different system configurations and the system with the configuration of $\alpha_1 = 0$, $\alpha_2 = 1$, $r_{S_1} = 1$ and $r_{S_2} = 0$ yields the lowest system throughput among the four different system configurations. This indicates that in our simulated system, the group 1 has much greater impact on contributing information rate to the system throughput. Moreover, it also shows that the system with the configuration of $\alpha_1 = 1$, $\alpha_2 = 0$, $r_{S_1} = 0$ and $r_{S_2} = 1$ and the system with the configuration of $\alpha_1 = 1$, $\alpha_2 = 1$, $r_{S_1} = 1$ and $r_{S_2} = 1$ achieves the same system throughput. This also indicates that in our simulated system, group 1 has much greater impact on contributing information rate to the system throughput.

To discuss the effect of relay position on system performance, in Figure 4.10, we simulate the WSR versus different relay locations. In the simulations, we consider

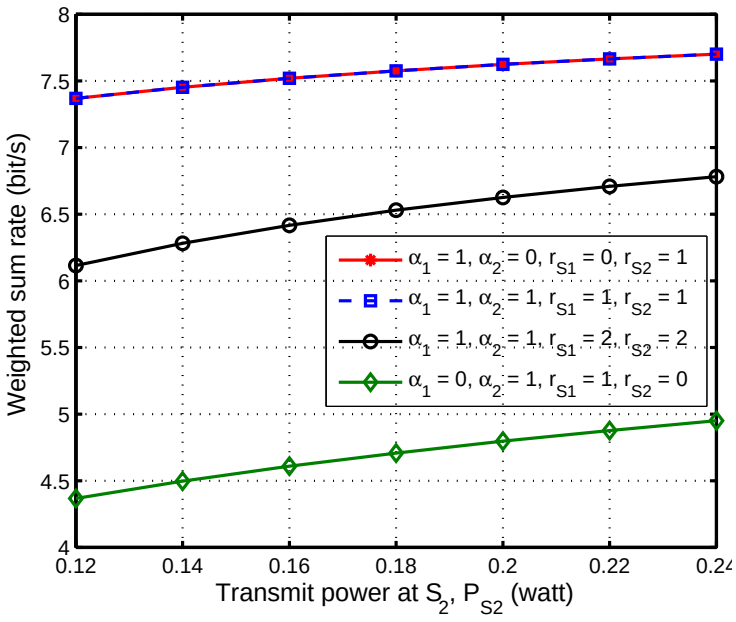

Figure 4.9: Weighted sum rate vs P_{S_2} for different α_1, α_2, r_{S_1} and r_{S_2}

such a network topology as shown in Figure 4.12, where S_2 is located at the origin of the coordination, D_2 is located at the point with coordinate $(x = 10, y = 0)$ on the $x - y$ plane, S_1 is positioned at $(x = 5, y = 5)$ and D_2 is placed at $(x = 10, y = 5)$. The position of R is changed within the region of $1 \leq x \leq 9$ and $0 \leq y \leq 4$. From the result in Figure 4.10, it can be seen that the relay should be positioned closer to S_1 for better system performance. When it is closer to S_2, the system achieves relatively low weighted sum rate. In order to show this more clearly, the contour lines associated with Figure 4.10 are provided by Figure 4.11.

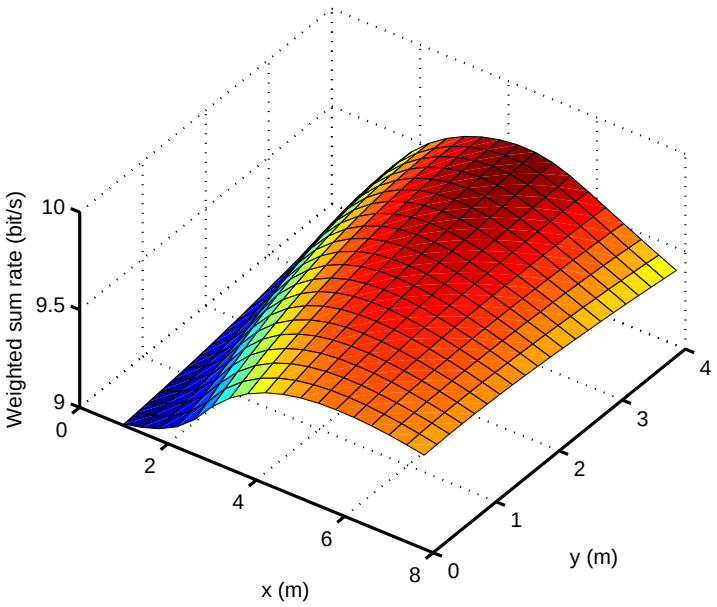

Figure 4.10: Weighted sum rate vs different relay positions

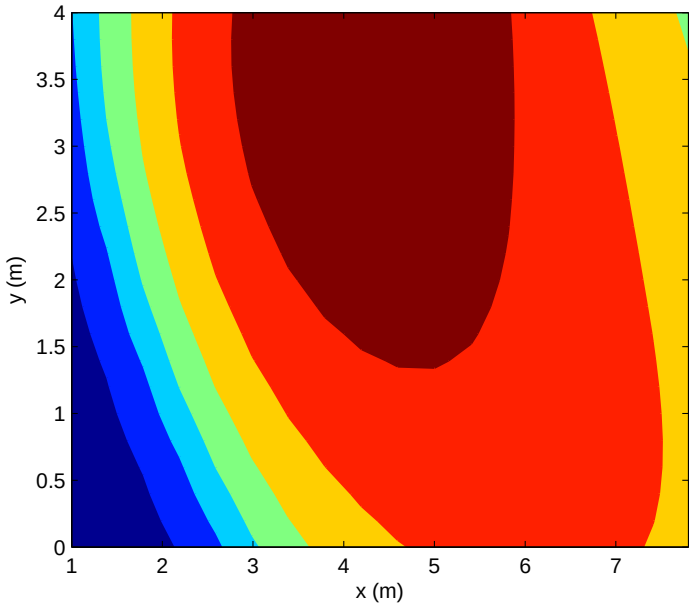

Figure 4.11: Contour lines of weighted sum rate vs different relay positions

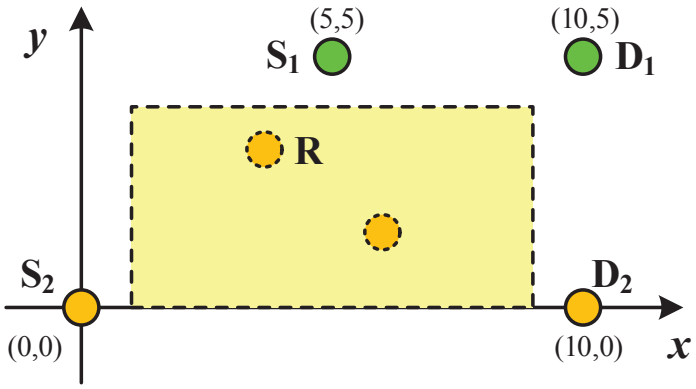

Figure 4.12: Simulation illustration for the relay positions on $x-y$ coordinate plane.

4.3.2 Simulations for Average Power Constrained Scenario

In this section, the average power constrained scenario is simulated, where, for comparison, the equal time assignment with only beamforming optimization is simulated as a benchmark. Besides, the results associated with the fixed power scenario are also plotted for comparison.

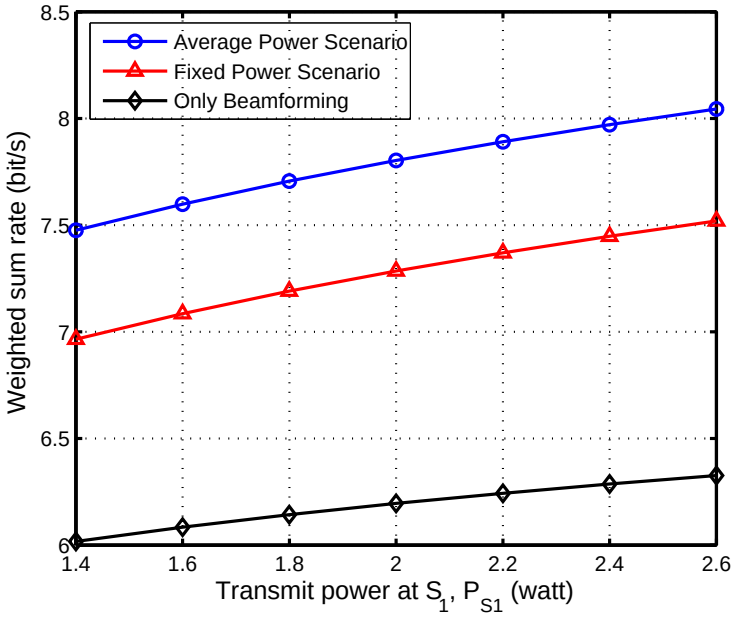

Figure 4.13: Weighted sum rate vs P_{S_1}.

In Figure 4.13, the WSR of the three schemes versus P_{S_1} are presented. It can be seen that, with the increment of P_{S_1}, the WSR of all the three schemes increase. It is due to that more power will bring higher information rate. It also can be observed that the average power constrained system has higher WSR than the fixed power constrained system and the benchmark system. The reason is that in the average power constrained system, S_1 has more flexibility in allocating power in its different transmitting phases.

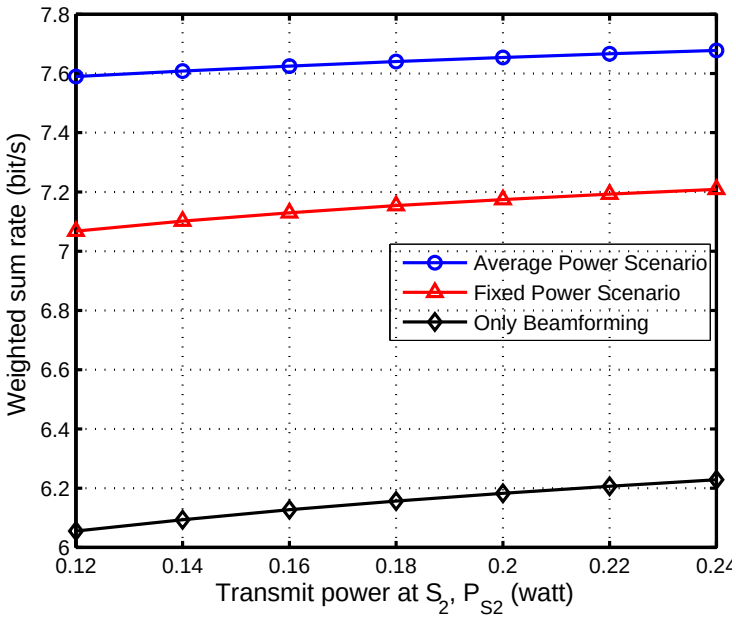

Figure 4.14: Weighted sum rate vs P_{S_2}.

Figure 4.14 plots the WSRs of the three schemes versus P_{S_2}. It also can be seen that with the increment of P_{S_2}, the system performances of the three methods increase. Similar to the results in Figure 4.13, the average power constrained system outperforms the other two schemes.

In Figure 4.15 and 4.16, the normalized performance gain versus P_{S_1} and P_{S_2} are respectively provided. In the two figures, the WSRs of the average power constrained system and fixed power system are divided by the corresponding WSR of the benchmark system. In Figure 4.15, it shows that the normalized gains of the average power constrained system and the fixed power system increase with the increment of P_{S_1}. In Figure 4.4, the normalized gain of the average power constrained scenario increases while in Figure 4.4 the normalized gain of the fixed power scenario decreases with the increment of P_{S_2}. Moreover, it shows that in our

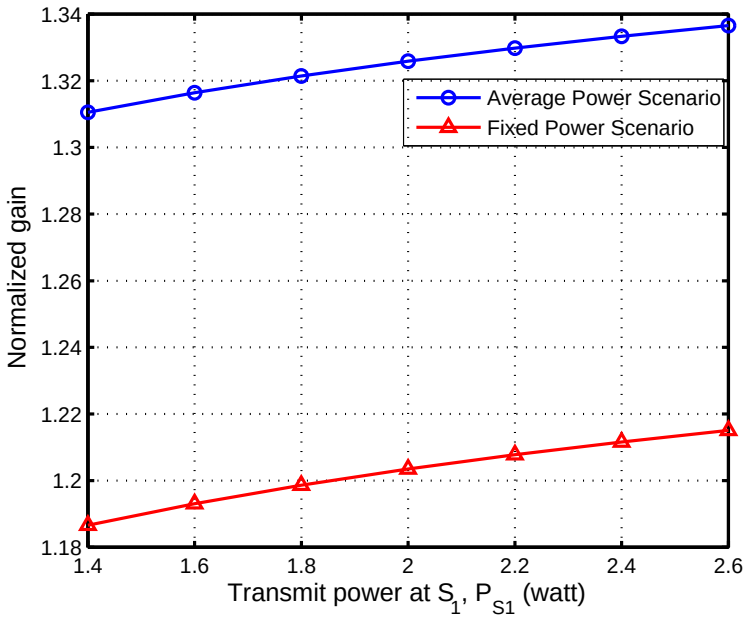

Figure 4.15: Normalized gain vs P_{S_1}.

numerical experiments, for a given P_{S_1}, the average power constrained system is able to improve the system WSR at least 1.3 times that of the benchmark system and for a given P_{S_2}, it improves the system WSR at most 1.3 times that of the benchmark system. This means that increasing either P_{S_1} or P_{S_2} may enhance the system performance, but increasing P_{S_1} can bring much greater performance gain for the system.

In Figure 4.17, we simulate the same dynamic scenario as in Figure 4.1. D_1 is moving away from S_1 along the line of $S_2 - D_2$ line. We desire to evaluate the impact of the distance $d_{S_1D_1}$ on system performance. It can be seen that with the increment of $d_{S_1D_1}$, the weighted sum rate is decreasing.

In the Figure 4.18, the WSR is plotted versus the number of antennas equipped at S_1. Similar to the situation of the fixed power system, with the increment of

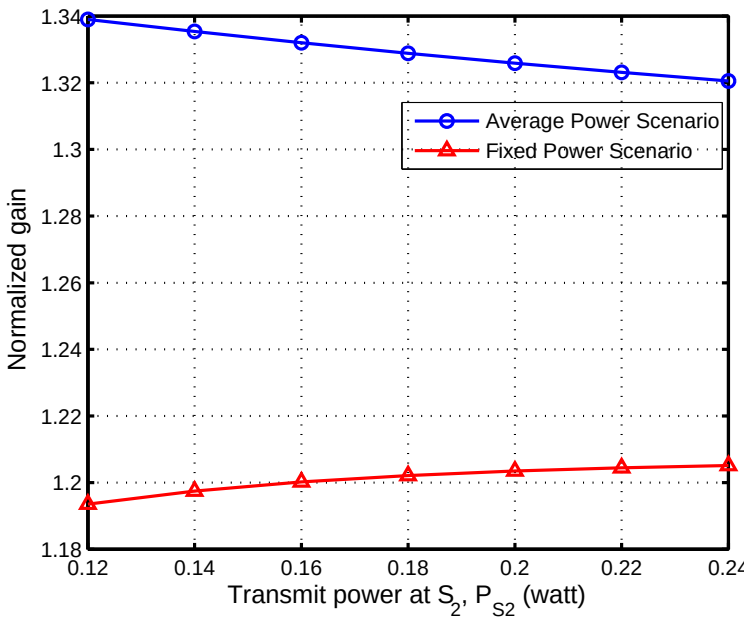

Figure 4.16: Normalized gain vs P_{S_2}.

number of antennas, the system performance can also be improved. However, with the increment of the number of antennas, the increasing rate of the weighted sum rate roughly decreases, which means that increasing the number of antennas can enhance system performance, but cannot increase the system performance infinitely.

We also discuss the effect of weights and the thresholds of the minimal required data rates on system performances by considering two different system configurations as presented in Figure 4.19 and 4.20. One is with the parameter setting of $\alpha_1 = 0$, $r_{S_2} = 0$, which guarantees the minimal required data rate of the bandwidth-limited user S_1. The other is with the parameter setting of $\alpha_2 = 0$, $r_{S_1} = 0$, which guarantees the minimal required data rate of the power-limited user S_2. Figure 4.19 and 4.20 provide some numerical results of the system performance associated with different α_1, α_2, r_{S_1} and r_{S_2} versus P_{S_1} and P_{S_2}, respectively. From the two Figures,

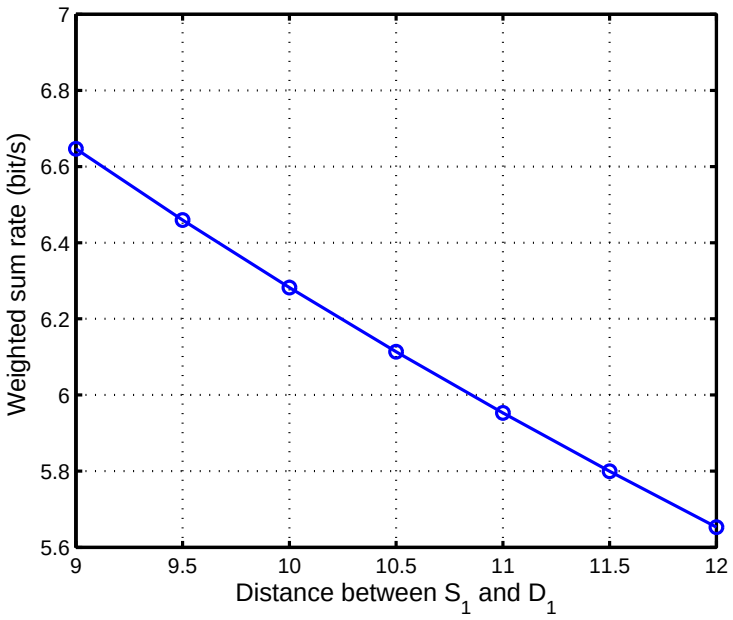

Figure 4.17: Weighted sum rate vs $d_{S_1D_1}$.

it can be observed that the system with the configuration of $\alpha_1 = 1$, $\alpha_2 = 1$, $r_{S_1} = 1$ and $r_{S_2} = 1$ yields the highest system throughput among the four different system configurations and the system with the configuration of $\alpha_1 = 0$, $\alpha_2 = 1$, $r_{S_1} = 2$ and $r_{S_2} = 0$ yields the lowest system throughput among the four different system configurations. This indicates that in our simulated system, the group 1 has much greater impact on contributing information rate to the system throughput. Moreover, it also shows that the system with the configuration of $\alpha_1 = 1$, $\alpha_2 = 0$, $r_{S_1} = 0$ and $r_{S_2} = 1$ and the system with the configuration of $\alpha_1 = 1$, $\alpha_2 = 1$, $r_{S_1} = 1$ and $r_{S_2} = 1$ achieves the same system throughput. This also indicates that in our simulated system, the group 1 has much greater impact on contributing information rate to the system throughput.

To discuss the effect of relay position on system performance, in Figure 4.21, we

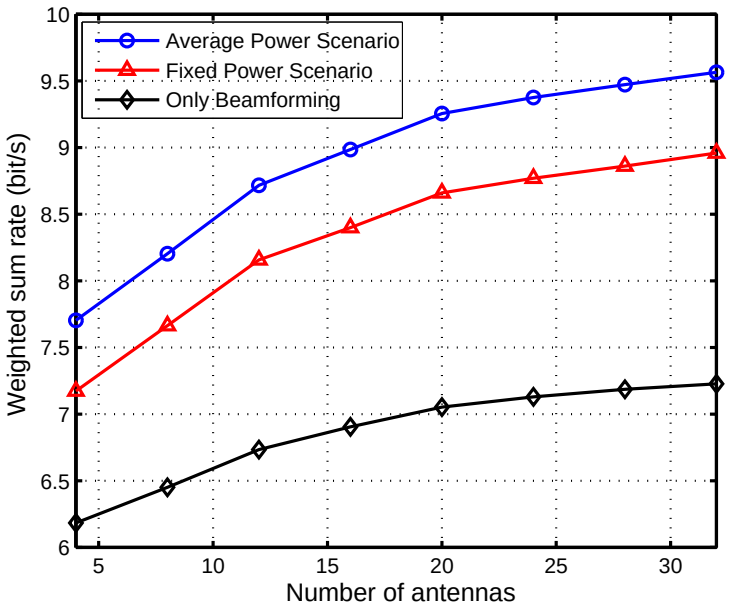

Figure 4.18: Weighted sum rate vs number of antennas.

simulate the WSR versus different relay locations. The simulated network topology is the same with that used for Figure 4.10. From Figure 4.21, it can be seen that the relay should be positioned closer to S_1 for achieving better system performance. When it is closer to S_2, the system achieves relatively low WSR. In order to show this more clearly, the contour lines associated with Figure 4.21 are provided by Figure 4.22.

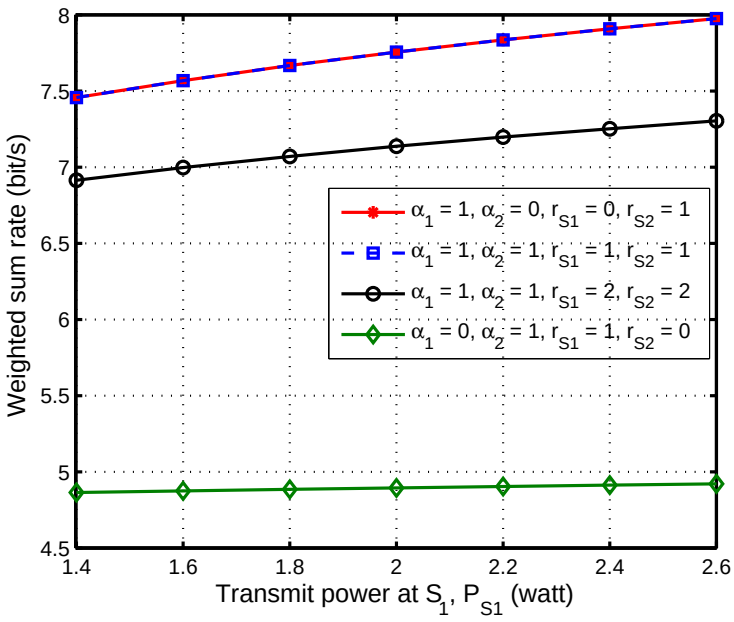

Figure 4.19: Weighted sum rate vs P_{S_1} for different α_1, α_2, r_{S_1} and r_{S_2}

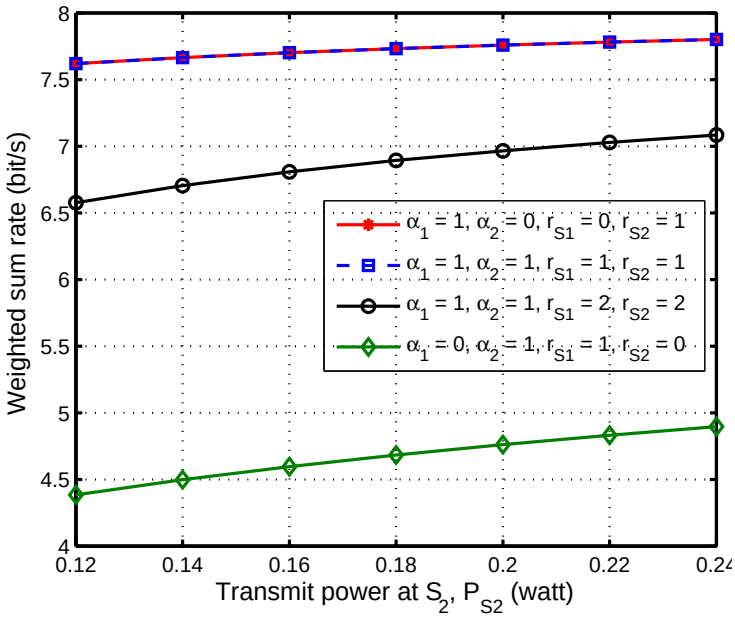

Figure 4.20: Weighted sum rate vs P_{S_2} for different α_1, α_2, r_{S_1} and r_{S_2}

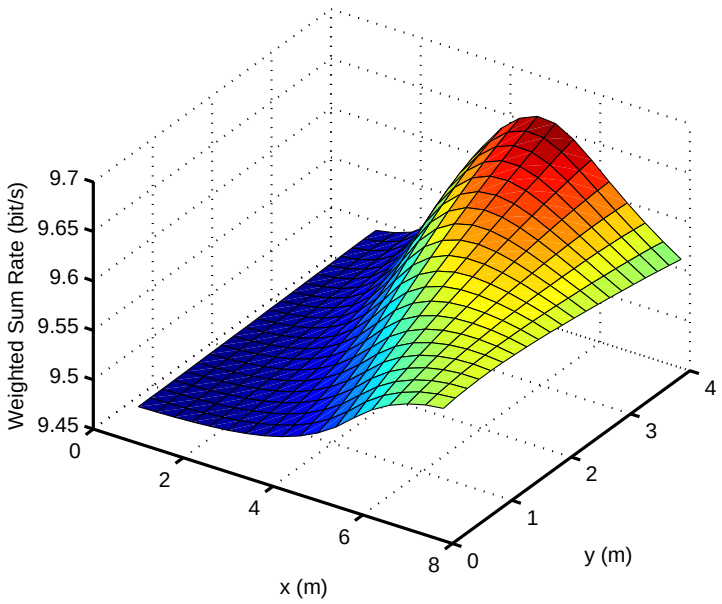

Figure 4.21: Weighted sum rate vs different relay positions

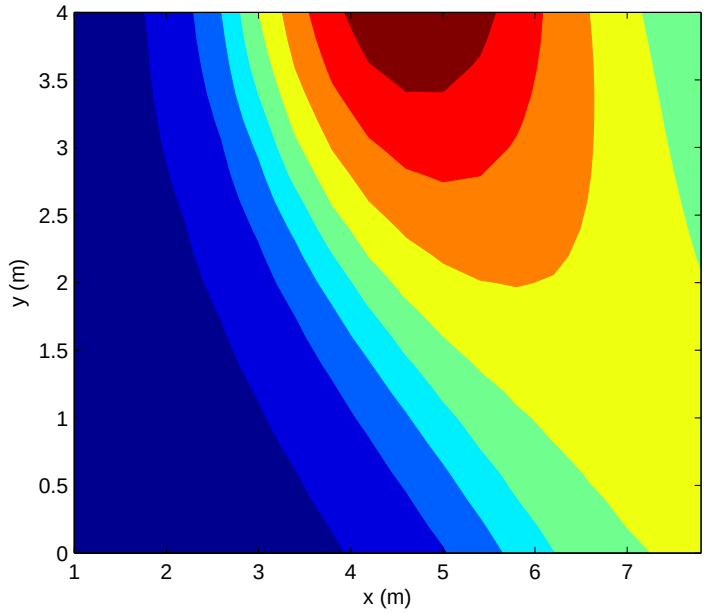

Figure 4.22: Contour lines for weighted sum rate vs different relay positions

Chapter 5: Total Power Minimization Design

Besides the throughput maximization design, in energy-constrained wireless networks, e.g., WSNs, WPANs and WBANs, the energy-saving design is also a critical objective for practical systems. Therefore, in this section, we consider the minimum energy consumption design for the wireless powered system described in Chapter 3. Our goal is to jointly optimize the energy beamforming and time allocation to minimize the total consumed power while guaranteeing the required information rates of the two groups.

5.1 Problem Formulation

The required minimum information rate constraints described in (4.1) are also considered. As described in Chapter 3, S_1 transmits signals in the first and the fourth phases, while S_2 transmits signals only in the second phase. Specifically, in the first phase, the consumed energy at S_1 is $\tau_1\|\mathbf{w}\|^2$. In the fourth phase, the consumed energy at S_1 is $\tau_4 P_{S_1}^{(4)}$. In the second phase, the consumed energy at S_2 is $\tau_2 P_{S_2}^{(2)}$. As a result, the total consumed energy for a fading block is $\tau_1\|\mathbf{w}\|^2 + \tau_4 P_{S_1}^{(4)} + \tau_2 P_{S_2}^{(2)}$. Since the time period T of the fading block is normalized to be 1, the total consumed

power for the transmissions in the fading block is

$$P_{avg} = \tau_1 \|\mathbf{w}\|^2 + \tau_4 P_{S_1}^{(4)} + \tau_2 P_{S_2}^{(2)}. \tag{5.1}$$

The total power minimization problem can be formulated as

$$\begin{aligned} \mathbf{P}_3 : \underset{\boldsymbol{\tau},\mathbf{w},\mathbf{P}}{\text{minimize}} \quad & \tau_2 P_{S_2}^{(2)} + \tau_1 \|\mathbf{w}\|^2 + \tau_4 P_{S_1}^{(4)} \\ \text{subject to} \quad & (3.1), (3.6), (3.11), \\ & (3.10), (3.13), (4.1), \end{aligned}$$

which is not jointly convex w.r.t. $\boldsymbol{\tau}$, $\mathbf{w}$ and $\mathbf{P}$ due to constraints (3.10) and (4.1), it also has no known solution method. Therefore, we solve it as follows.

5.2 Problem Transformation and Solution

If we use a similar transformation, i.e., $\mathbf{W} = \mathbf{w}\mathbf{w}^H$ as described in chapter 4, constraints (3.10), (3.6) and (3.13) of Problem $\mathbf{P}_3$ also can be equally replaced by (4.6), (4.19) and (4.20), respectively. And, its objective function as shown in (5.1) can be rewritten to be

$$P_{avg} = \tau_2 P_{S_2}^{(2)} + \tau_1 \mathrm{Tr}(\mathbf{W}) + \tau_4 P_{S_1}^{(4)}. \tag{5.2}$$

In order to equivalently transform Problem $\mathbf{P}_3$ into the following Problem $\mathbf{P}_3'$, $\mathbf{W}$ must be semi-definite and rank one, as expressed by the constraints (4.9) and (4.10). Thus, Problem $\mathbf{P}_3'$ then can be given by

$$\begin{aligned} \mathbf{P}_3' : \underset{\boldsymbol{\tau},\mathbf{W},\mathbf{P}}{\text{minimize}} \quad & \tau_2 P_{S_2}^{(2)} + \tau_1 \mathrm{Tr}(\mathbf{W}) + \tau_4 P_{S_1}^{(4)} \\ \text{subject to} \quad & (3.1), (3.11), (4.1), (4.6), \\ & (4.9), (4.10), (4.19), (4.20). \end{aligned}$$

Since Problem $\mathbf{P}_3'$ is still non-convex, we further transform it to be the following Problem $\mathbf{P}_3''$ by defining

$$\begin{cases} \mathbf{V} = & \tau_1 \mathbf{W}, \\ \phi_1 = & \tau_3 P_R, \\ \phi_2 = & \tau_2 P_{S_2}^{(2)}, \\ \phi_3 = & \tau_1 P_{S_1}^{(1)}, \\ \phi_4 = & \tau_4 P_{S_1}^{(4)}, \end{cases} \tag{5.3}$$

which is similar to (4.21).

To make Problem $\mathbf{P}_3''$ be an equivalent version of Problem $\mathbf{P}_3'$, $\mathbf{V}$ also should satisfy the semi-definite constraint and rank-one constraint, which can be expressed by (4.11) and (4.12). Moreover, with (5.3), constraints (4.6), (3.11), (4.19) and (4.20) are replaced with (4.15), (4.22), (4.25) and (4.26) respectively. The objective function (5.2) of Problem $\mathbf{P}_3'$ can be transformed into

$$P_{avg} = \phi_2 + \mathrm{Tr}(\mathbf{V}) + \phi_4. \tag{5.4}$$

As a result, Problem $\mathbf{P}_3''$ can be given by

$$\begin{aligned} \mathbf{P}_3'' : \underset{\boldsymbol{\tau}, \mathbf{V}, \boldsymbol{\phi}}{\text{minimize}} \quad & \phi_2 + \mathrm{Tr}(\mathbf{V}) + \phi_4 \\ \text{subject to} \quad & (3.1), (4.1), (4.11), (4.12), \\ & (4.15), (4.22), (4.25), (4.26). \end{aligned}$$

It can be seen that the objective function of Problem $\mathbf{P}_3''$ is convex and all constraints except the rank-one constraint (4.12) are convex sets. Therefore, by using SDR method with the dropping of (4.12), Problem $\mathbf{P}_3''$ can be relaxed to a

convex problem as follows,

$$\begin{aligned} \mathbf{P}_3''' : \underset{\boldsymbol{\tau},\mathbf{V},\boldsymbol{\phi}}{\text{minimize}} \quad & \phi_2 + \text{Tr}(\mathbf{V}) + \phi_4 \\ \text{subject to} \quad & (3.1), (4.1), (4.11), \\ & (4.15), (4.22), (4.25), (4.26). \end{aligned}$$

Hence, the optimal solution $[\boldsymbol{\tau}^*, \mathbf{V}^*, \boldsymbol{\phi}^*]$ of Problem $\mathbf{P}_3'''$ can be obtained by using some known solution methods.

As is known, with SDR method, only when $\text{rank}(\mathbf{V}^*) = 1$, $[\boldsymbol{\tau}^*, \mathbf{V}^*, \boldsymbol{\phi}^*]$ is also the optimal solution of Problem $\mathbf{P}_3''$. In this case, the optimal $[\boldsymbol{\tau}^*, \mathbf{w}^*, \mathbf{P}^*]$ can be derived accordingly. Therefore, the key question lies in the rank of $\mathbf{V}^*$. Fortunately, we also found that $\text{rank}(\mathbf{V}^*) = 1$ always holds for Problem $\mathbf{P}_3'''$, which means the global optimum of the primary Problem $\mathbf{P}_3$ also can be guaranteed by our adopted variable substitutions and SDR.

Now we analyse the rank of $\mathbf{V}^*$ for the minimum average power design with Theorem 5.1.

Theorem 5.1. *There exists an optimal* $\mathbf{V}^*$ *of Problem* $\mathbf{P}_3'''$ *such that rank*$(\mathbf{V}^*) = 1$.

Proof. First, we apply the substitution

$$\text{Tr}(\mathbf{V}) = t, \tag{5.5}$$

on Problem $\mathbf{P}_3'''$ and get an equivalent Problem $\mathbf{G}$,

$$\begin{aligned} \mathbf{G} : \underset{\boldsymbol{\tau},\mathbf{V},\boldsymbol{\phi},t}{\text{minimize}} \quad & \phi_2 + t + \phi_4 \\ \text{subject to} \quad & (3.1), (4.1), (4.11), (4.15), \\ & (4.22), (4.25), (4.26), (5.5). \end{aligned}$$

Next, we consider the following Problem $\mathbf{Q}_3$,

$$\begin{aligned}
\mathbf{Q}_3: \underset{\mathbf{U}}{\text{minimize}} \quad & \text{Tr}(\mathbf{U}) \\
\text{subject to} \quad & \phi_1^* \leq \eta \text{Tr}(\mathbf{U}\mathbf{h}_{S_1R}\mathbf{h}_{S_1R}^H), \\
& R_{S_1}^* = \tau_1^* \mathcal{C}\left(\frac{\text{Tr}(\mathbf{U}\mathbf{h}_{S_1D_1}\mathbf{h}_{S_1D_1}^H)}{N_0\tau_1^*}\right) + \tau_4^* \mathcal{C}\left(\frac{\phi_4^* \|\mathbf{h}_{S_1D_1}\|^2}{N_0\tau_4^*}\right), \\
& \text{Tr}(\mathbf{U}) = t^*, \\
& \mathbf{U} \succeq 0,
\end{aligned}$$

where τ_1^*, τ_4^*, ϕ_1^*, ϕ_4^*, t^* and $R_{S_1}^*$ are optimal solutions of Problem $\mathbf{G}$. Problem $\mathbf{Q}_3$ is equivalently transformed into Problem $\mathbf{Q}_3'$,

$$\begin{aligned}
\mathbf{Q}_3': \underset{\mathbf{U}}{\text{minimize}} \quad & \text{Tr}(\mathbf{U}) \\
\text{subject to} \quad & \text{Tr}(\mathbf{U}\mathbf{h}_{S_1R}\mathbf{h}_{S_1R}^H) \geq \frac{\phi_1^*}{\eta}, \\
& \text{Tr}(\mathbf{U}\mathbf{h}_{S_1D_1}\mathbf{h}_{S_1D_1}^H) = N_0\tau_1^* \left(2^{\frac{R_{S_1}^* - \tau_4^* \mathcal{C}\left(\frac{\phi_4^* \|\mathbf{h}_{S_1D_1}\|^2}{N_0\tau_4^*}\right)}{\tau_1^*}} - 1\right), \\
& \text{Tr}(\mathbf{U}) = t^*, \\
& \mathbf{U} \succeq 0,
\end{aligned}$$

According to Lemma 4.1, Problem $\mathbf{Q}_3$ has an optimal solution $\mathbf{U}^*$ which satisfies that

$$\text{rank}^2(\mathbf{U}^*) \leq 3.$$

Since $\text{rank}(\mathbf{U}^*) \neq 0$, we conclude that $\text{rank}(\mathbf{U}^*) = 1$.

Let $[\boldsymbol{\tau}^*, \mathbf{V}^*, \boldsymbol{\phi}^*, t^*]$ be the optimal solution of Problem $\mathbf{G}$. It can be inferred that $\mathbf{V}^*$ is a feasible solution of Problem $\mathbf{Q}_3$. The reason is that $[\boldsymbol{\tau}^*, \mathbf{V}^*, \boldsymbol{\phi}^*, t^*]$ also satisfy the constraints (4.15), (4.26) and (5.5). The optimal value of Problem $\mathbf{Q}_3$

associated with $\mathbf{U}^*$ must be smaller than that associated with any other feasible solution. Therefore, $\mathrm{Tr}(\mathbf{U}^*) \leq \mathrm{Tr}(\mathbf{V}^*) \leq \phi_3^*$.

If we construct a new tuple $[\boldsymbol{\tau}^*, \mathbf{U}^*, \boldsymbol{\phi}^*, t^*]$, then it satisfy all constraints of Problem **G**, which means it is a feasible solution of Problem **G**. Since the objective function of Problem **G** is only related to $\boldsymbol{\tau}$, $\boldsymbol{\phi}$ and t. $[\boldsymbol{\tau}^*, \mathbf{U}^*, \boldsymbol{\phi}^*, t^*]$ and $[\boldsymbol{\tau}^*, \mathbf{V}^*, \boldsymbol{\phi}^*, t^*]$ yield the same value of Problem **G**, which means that $[\boldsymbol{\tau}^*, \mathbf{U}^*, \boldsymbol{\phi}^*, t^*]$ is also an optimal solution of Problem **G**. Since we have proved that $\mathrm{rank}(\mathbf{U}^*) = 1$, we conclude that **G** has an optimal rank-one solution. We also know that Problem $\mathbf{P}_3'''$ is equivalent to Problem **G**. So $\mathbf{P}_3'''$ also has an optimal rank-one solution. □

Remark 5.1. *The optimal solution of Problem* $\mathbf{P}_3$ *is guaranteed to be found.*

The reason for Remark 5.1 is explained as follows. $\mathbf{P}_3$, $\mathbf{P}_3'$ and $\mathbf{P}_3''$ are equivalent to each other. It is known that once the optimal solution of $\mathbf{P}_3'''$ satisfies the rank-one constraint, it is equivalent to $\mathbf{P}_3$, $\mathbf{P}_3'$ and $\mathbf{P}_3''$. Theorem 5.1 declares that $\mathbf{P}_3'''$ has a rank-one optimal solution. Therefore, the optimal solution for Problem $\mathbf{P}_3$ can always be found by using our proposed solution method.

5.3 Simulations

In this section, we provide some simulation results to discuss the system performance of the total power minimization design. The simulations are performed on the same topology and parameters as described in Chapter 4. For comparison, we also simulate one benchmark system, in which equal time assignment is adopted, i.e., $\tau_1 = \tau_2 = \tau_3 = \tau_4 = 0.25$, and only beamforming vector $\mathbf{w}$ is optimized.

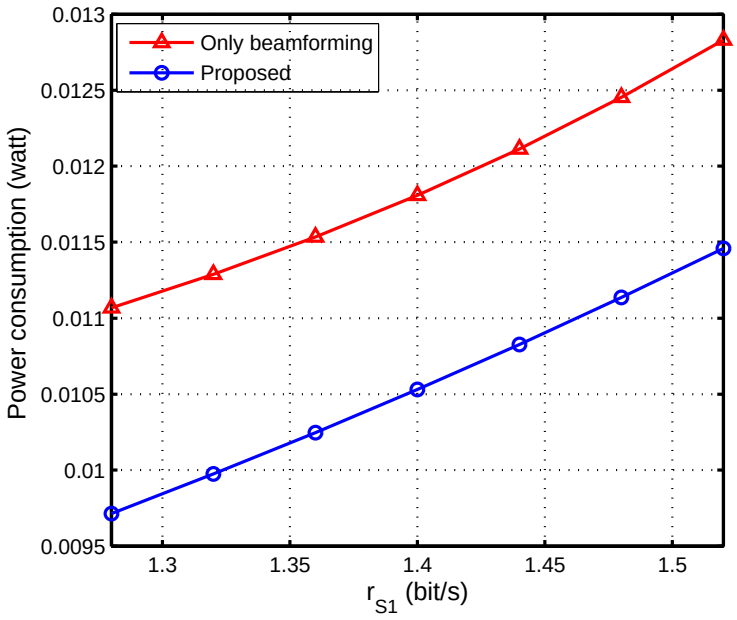

Figure 5.1: Minimal power consumption vs r_{S_1}.

Figure 5.1 and Figure 5.2 plot the minimal consumed power of the system versus r_{S_1} and r_{S_2}, respectively. It is shown that with the growth of the required information rate r_{S_1} and r_{S_2}, the total power consumption of the system also increases. This fits well with the intuition that to achieve higher information rate, more power is required.

To get more insights, in Figure 5.3 and Figure 5.4, we present the normalized performance gain of our proposed method to the benchmark system versus r_{S_1} and r_{S_2}, respectively. In Figure 5.3, it can be seen that with the increment of r_{S_1}, the power consumed by our proposed method increases, and it gradually approaches to that consumed by the benchmark system. In Figure 5.4, it is observed that with the increment of r_{S_2}, the power consumed by our proposed method increases much slower than that of the benchmark system. This observation is much different from

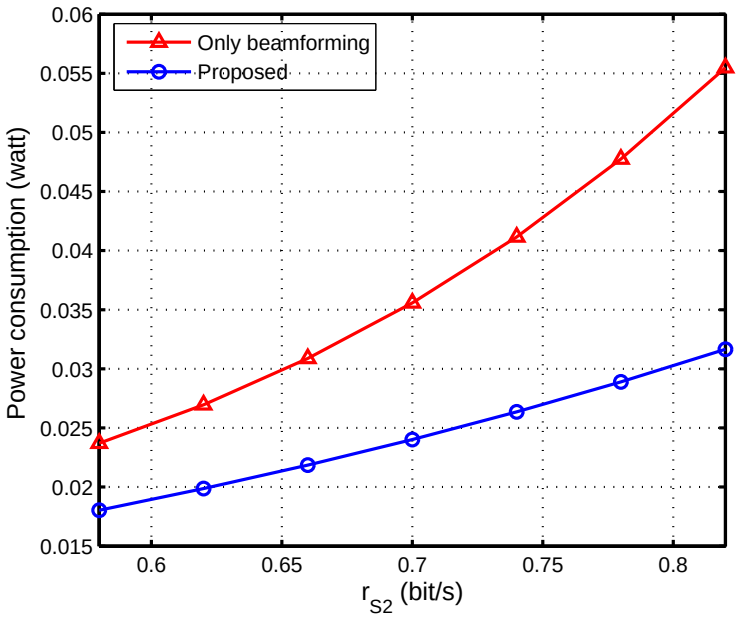

Figure 5.2: Minimal power consumption vs r_{S_2}.

the results in Figure 5.3. Combining the results in Figure 5.3 and Figure 5.4, it also can be inferred that, in our considered system, group 1 has much greater impact on system power consumption.

We also simulate the similar scenario described in Figure 4.6 to discuss the effect of $d_{S_1D_1}$ on system performance of the minimum power design. In Figure 5.5, one can see that as D_1 is moving away from S_1, more power is needed to ensure the system to get the required information rate. It is also observed that the slope of the consumed power is becoming higher with the growth of $d_{S_1D_1}$. It means that with the same amount of increment of $d_{S_1D_1}$, to guarantee the required data rates of the two groups, more power are required as $d_{S_1D_1}$ increases.

In Figure 5.6, the system performance versus the number of antennas is plotted. It can be seen that more antennas is able to reduce the power consumption of

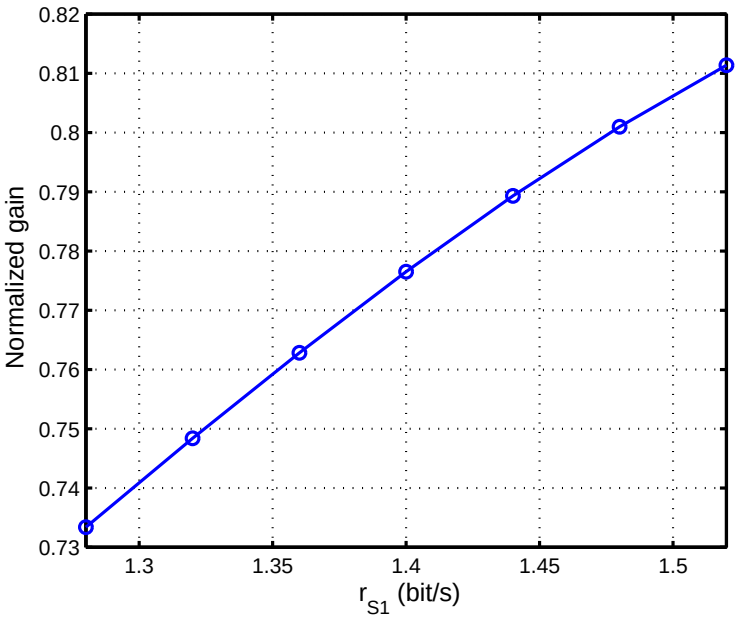

Figure 5.3: Normalized gain vs r_{S_1}.

the system. However, it also shows that the reduction of power decreases with the increment of number of antennas. This indications that by installing more antennas, the consumed power can be saved but it cannot reduce the power consumption infinitely.

To discuss the effect of relay position on system performance, in Figure 5.7, we simulate the minimum consumed power versus different relay locations. The network topology is the same as in Figure 4.10. From the results in Figure 5.7, it can be seen that the relay should be positioned closer to S_1 for achieving less power consumption. When it is closer to S_2, the system consumes relatively high power. In order to show this more clearly, the contour lines associated with Figure 5.7 are provided by Figure 5.8.

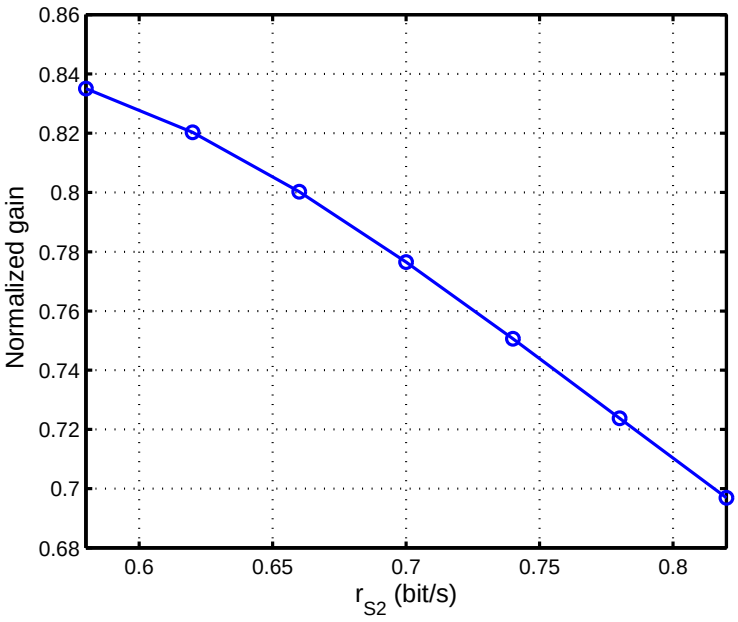

Figure 5.4: Normalized gain vs r_{S_2}.

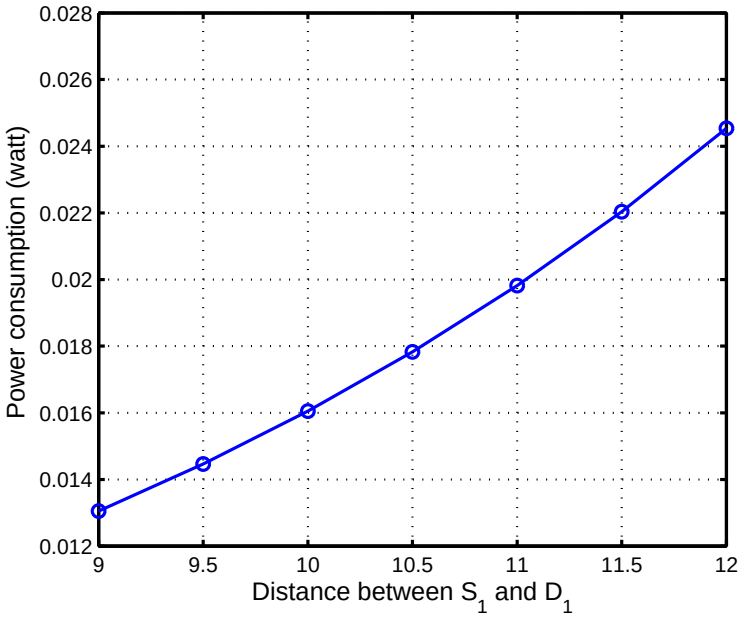

Figure 5.5: Minimal power consumption vs $d_{S_1D_1}$.

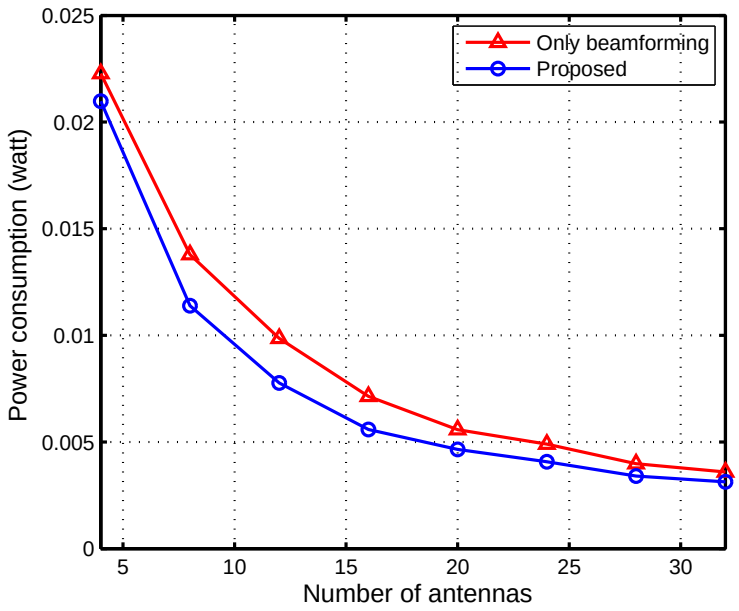

Figure 5.6: Minimal power consumption vs number of antennas.

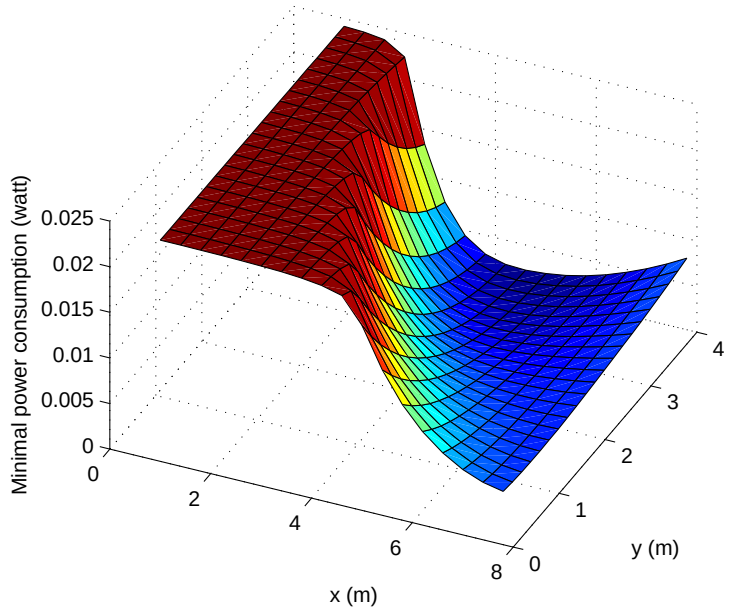

Figure 5.7: Minimal power consumption vs different relay positions

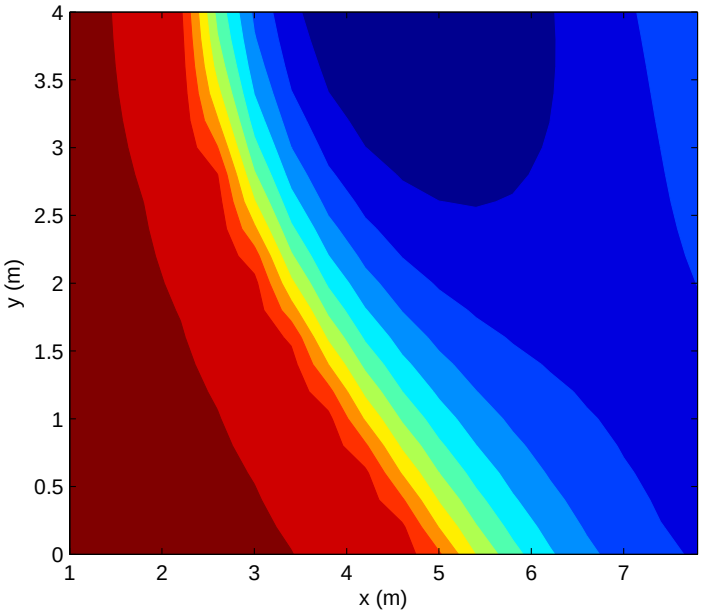

Figure 5.8: Contour lines for minimal power consumption vs different relay positions

Chapter 6: Conclusion

This work focused on the optimal WPCN design. A network composed of two communication groups was considered, where the first group has sufficient power supply but no available bandwidth, and the second group has licensed bandwidth but very limited power to perform required information transmission. For such a system, we introduced the power and bandwidth cooperation between the two groups so that both group can accomplish their expected information delivering tasks. We proposed a cooperative transmission protocol for the considered system, where group 1 transmits some power to group 2 to help group 2 with information transmission and then group 2 gives some bandwidth to group 1 in return. To explore the information transmission performance limit of the system, we formulated two optimization problems to maximize the system WSR by jointly optimizing the time assignment, power allocation, and energy beamforming under different power constraints, i.e., the fixed power constraint and the average power constraint. In order to make the cooperation between the two groups meaningful and guarantee the QoS requirements of both groups, the minimal required data rates of the two groups were considered as constraints for the optimal system design. As both problems were non-convex and have no known solutions, we solved them by using proper

variable substitution and the SDR. We theoretically proved that our proposed solution method can guarantee to find the global optimal solution. Besides, we also investigated the minimal power consumption optimal design for the considered cooperation WPCN. We formulated an optimization problem to minimize the total consumed power by jointly optimizing the time assignment, power allocation, and energy beamforming under required data rate constraints. As the problem is also non-convex and has no known solutions, we solved it by using some variable substitutions and the SDR method. We also theoretically proved that our proposed solution method for the minimal power consumption design guarantees the global optimal solution. Extensive experimental results were provided to discuss the system performance behaviors, which provided some useful insights for future WPCN design. It shows that the average power constrained system achieves higher weighted sum rate than the fixed power constrained system. Besides, it also shows that in such a WPCN, relay should be placed closer to the multi-antenna hybrid access point to achieve higher weighted sum rate and consume lower total power.

For our considered system, besides the work we have done in this thesis, some other problems are also deserved to be investigated in future. Firstly, in current work, only S_1 is equipped with multiple antennas. How to extend the obtained results to a more general and complex scenario where all nodes are installed multiple antennas is an interesting problem. Secondly, in current work, R is only employed to help the information transmission for group 2. Actually, it also can be employed to help the information transmission for group 1. Wether the system performance can be further improved when R is also used to help the information transmission for

group 1 is another interesting problem. Thirdly, in in current work, we adopted the harvest-and-use transmission protocol. If R has some energy storage requirement or limitation, how about the optimal design of the new evolved system?

Bibliography

[1] X. Lu et al., "reless networks with RF energy harvesting: A contemporary survey," *IEEE Commun. Surveys and Tutorials*, vol. 17, no. 2, pp. 757C789, Secondquarter 2015.

[2] S. Bi, C. K. Ho, and R. Zhang, Wireless powered communication: opportunities and challenges, IEEE Commun. Mag., vol. 53, no. 4, pp. 117C125, Apr. 2015.

[3] S. Z. Bi, Y. Zeng, R. Zhang, "Wireless powered communication networks: an overview," *IEEE Wireless Communications,* Vol. 23, no. 2, pp. 10 - 18, 2016.

[4] Butt, M. Majid, et al. "RF Energy Harvesting Communications: Recent Advances and Research Issues" *Energy Management in Wireless Cellular and Adhoc Networks*. Springer International Publishing, 339-363, 2016.

[5] M. L. Ku, W. Li, Y. Chen, and K.J.R. Liu, "Advances in Energy Harvesting Communications: Past, Present, and Future Challenges", IEEE Communications Surveys and Tutorials, vol 18, no 2, pp.1384 - 1412, May 2016.

[6] Y. H. Suh and K. Chang, "A High-Efficiency Dual-Frequency Rectenna for 2.45- and 5.8-GHz Wireless Power Transmission," IEEE Trans. Microwave Theory and Techniques, vol. 50, no. 7, pp. 1784C89, July 2002.

[7] R. Madan et al., "Energy-efficient cooperative relaying over fading channels with simple relay selection," IEEE Trans. Wireless. Commun., vol. 7, no. 8, pp. 3013C3025, Aug. 2008.

[8] C. K. Ho, P. H. Tan, and S. Sun, Energy-efficient relaying over multiple slots with causal CSI, IEEE J. Sel. Areas Commun., vol. 31, no. 8, pp. 1494C1505, Aug. 2013.

[9] K. Xiong, P. Fan, Y. Lu, K.B. Letaief, "Energy Efficiency with Proportional Rate Fairness in Multi-Relay OFDM Networks," *IEEE Jour. on Selected Areas in Communications*, vol. 34, no. 5, pp. 1431-1447, May 2016

[10] S. Ulukus, A. Yener, E. Erkip, O. Simeone, M. Zorzi, P. Grover and K. Huang, "Energy Harvesting Wireless Communications: A Review of Recent Advances," *IEEE Jour. on Selected Areas in Communications*, vol. 33, no. 3, pp. 360-381, March 2015.

[11] E. Ekrem and S. Ulukus, "Capacity-Equivocation Region of the Gaussian MIMO Wiretap Channel," *IEEE Trans. on Information Theory*, vol. 58, pp. 9, pp. 5699-5710, Sept. 2012.

[12] J. Yang and S. Ulukus, "Optimal Packet Scheduling in a Multiple Access Channel with Energy Harvesting Transmitters," *Journal of Communications and Networks*, special issue on Energy Harvesting in Wireless Networks, vol. 14, no. 2, pp. 140-150, April 2012.

[13] J. Yang, O. Ozel and S. Ulukus, "Broadcasting with an Energy Harvesting Rechargeable Transmitter," *IEEE Trans. on Wireless Communications*, vol. 11, no. 2, pp. 571-583, Feb. 2012.

[14] J. Yang and S. Ulukus, "Optimal Packet Scheduling in an Energy Harvesting Communication System," *IEEE Trans. on Communications*, vol. 60, no. 1, pp. 220-230, Jan. 2012.

[15] O. Ozel, K. Tutuncuoglu, J. Yang, S. Ulukus and A. Yener, "Transmission with Energy Harvesting Nodes in Fading Wireless Channels: Optimal Policies," *IEEE Jour. on Selected Areas in Communications*, vol. 29, no. 8, pp. 1732-1743, Sept. 2011.

[16] A. Arafa and S. Ulukus, "Optimal Policies for Wireless Networks with Energy Harvesting Transmitters and Receivers: Effects of Decoding Costs," *IEEE Jour. on Selected Areas in Communications C Series on Green Communications and Networking*, vol.33, no. 12, pp. 2611-2625, December 2015.

[17] L. R. Varshney, "Transporting information and energy simultaneously," in *Proc. IEEE Int. Symp. Inf. Theory* (ISIT), pp. 1612-1616, July 2008.

[18] P. Grover and A. Sahai, "Shannon meets Tesla: wireless information and power transfer," in *Proc. IEEE Int. Symp. Inf. Theory (ISIT)*, pp. 2363-2367, June 2010.

[19] R. Zhang and C. K. Ho, "MIMO Broadcasting for Simultaneous Wireless Information and Power Transfer," *IEEE Trans. Wireless Commun.*, vol. 12, no. 5, pp. 1989C2001, May 2013.

[20] H. Ju and R. Zhang, "Throughput maximization in wireless powered communication networks," *IEEE Trans. Wireless Commun.*, vol. 13, no. 1, pp. 418-428, Jan. 2014.

[21] H. Ju and R. Zhang, "User cooperation in wireless powered communication networks," in *Proc. IEEE GLOBECOM*, Dec. 2014.

[22] X. Chen, C. Yuen, and Z. Zhang, "Wireless energy and information transfer tradeoff for limited feedback multi-antenna systems with energy beamforming," *IEEE Trans. Veh. Technol.*, vol. 63, no. 1, pp. 407-412, Jan. 2014.

[23] Q. Sun, G. Zhu, C. Shen, et al., "Joint Beamforming Design and Time Allocation for Wireless Powered Communication Networks," *IEEE Commun. Lett*, vol. 18, no. 10, pp. 1783-1786, Oct. 2014.

[24] H. Ju and R. Zhang, "Optimal Resource Allocation in Full-Duplex Wireless-Powered Communication Network," *IEEE Trans. on Communications*, VOL. 62, NO. 10, pp. 3528-3540, OCTOBER 2014.

[25] Y. L. Che, L. J. Duan and R. Zhang, "Spatial Throughput Maximization of Wireless Powered Communication Networks" *IEEE J. Sele. Areas Commun.*, vol. 33, no. 8, pp. 1534-1548, Aug. 2015

[26] S. H. Choi and D. I. Kim, "Backscatter Radio Communication for Wireless Powered Communication Networks," in *Proc. IEEE APCC'2015*, pp. 370-374, 2015.

[27] Y. L. Che, J. Xu, L. J. Duan and R. Zhang, "Multiantenna Wireless Powered Communication With Cochannel Energy and Information Transfer," *IEEE Communications Letters*, VOL. 19, NO. 12, pp. 2266-2269, DEC. 2015

[28] Q. Q. Wu, M. X. Tao, D. W. Kwan Ng, W. Chen, and R. Schober, "Energy-Efficient Transmission for Wireless Powered Multiuser Communication Networks," in *Proc. IEEE ICC*, pp. 154-159, 2015.

[29] Y. Y. Ma, H. (Henry) Chen, Z. H. Lin, Y. H. Li, and B. Vucetic, "Distributed Resource Allocation for Power Beacon-Assisted Wireless-Powered Communications," in *Proc. IEEE ICC*, pp. 3849-3854, 2015.

[30] Q. Z. Yao, A. P. Huang, H. G. Shan, T. Q. S. Quek, W. Wang, "Delay-Aware Wireless Powered Communication Networks - Energy Balancing & Optimization," early access in *IEEE Trans. Wireless Commun.*, vol. 99, no. 99, 2016

[31] S. Z. Bi,and Rui Zhang, "Placement Optimization of Energy and Information Access Points in Wireless Powered Communication Networks," *IEEE Trans. on Wireless Communications*, VOL. 15, NO. 3, pp. 2351-2364, MARCH 2016

[32] F. Zhao, L. Wei, and H. B. Chen, "Optimal Time Allocation for Wireless Information and Power Transfer in Wireless Powered Communication Systems," *IEEE Trans. on Vehicular Technology*, VOL. 65, NO. 3, pp. 1830-1835, MARCH 2016

[33] H. Lee, K.-J. Lee, H. J. Kim, B. Clerckx and I. Lee, "Resource Allocation Techniques for Wireless Powered Communication Networks With Energy Storage Constraint," *IEEE Trans. on Wireless Communications*, VOL. 15, NO. 4, pp. 2619-2628, APRIL 2016

[34] Hanjin Kim, Hoon Lee, Minki Ahn, Han-Bae Kong,and Inkyu Lee, "Joint Subcarrier and Power Allocation Methods in Full Duplex Wireless Powered Communication Networks for OFDM Systems," early access in *IEEE Trans. on Wireless Communications,* 2016.

[35] Zheng Zhou, Mugen Peng, Zhongyuan Zhao, Wenbo Wang, and Rick S. Blum, "Wireless-Powered Cooperative Communications: Power-Splitting Relaying With Energy Accumulation," *IEEE J. Sele. Areas Commun.*, vol. 34, no. 4, pp. 969-982, April 2016.

[36] N. Shinohara, "Power Without Wires," IEEE Microwave Mag., vol. 12, no. 7, pp. 564C73, Dec. 2011.

[37] X. Zhou, R. Zhang, and C. K. Ho, "Wireless Information and Power Transfer: Architecture Design and Rate-Energy Tradeoff," *IEEE Trans. Commun.*, vol. 61, no. 11, pp. 4754C67, Nov. 2013.

[38] J. N. Laneman, D. N. C. Tse, and G. W. Wornell, "Cooperative Diversity in Wireless Neworks: Efficient Protocols and Outage Behavior," *IEEE Trans. Inform. Theory*, vol. 50, no. 12, pp. 3062-3080, Dec. 2004.

[39] A. Chakrabarti, A. Sabharwal, and B. Aazhang, "Cooperative communications: Fundamental limits and practical implementation," in *Cooperation in Wireless Networks: Principles and Applications*, F. H. P. Fitzek and M. D. Katz, Eds. Springer, 2006.

[40] P. Liu, Z. Tao, Z. Lin, E. Erkip, and S. Panwar, "Cooperative Wireless communications: A Cross-Layer Approach," *IEEE Wireless Commun.*, vol. 13, no. 4, pp. 84-92, Aug. 2006.

[41] Tse, David, and Pramod Viswanath. *Fundamentals of wireless communication.* Cambridge university press, 2005.

[42] Huang, Yongwei, and Daniel P. Palomar, "Rank-constrained separable semidefinite programming with applications to optimal beamforming," *IEEE Trans. on Signal Processing*, vol. 58, no. 2, pp. 664-678, 2010.

[43] Boyd, Stephen, and Lieven Vandenberghe. *Convex optimization.* Cambridge university press, 2004.

[44] Luo, Zhi-Quan, et al, "Semidefinite relaxation of quadratic optimization problems," *IEEE Signal Processing Magazine* vol. 27, no. 3, 2010.